AN ATTITUDE ESTIMATION ALGORITHM FOR A FLOATED INERTIAL REFERENCE

by

Stephen G. Sifferlen

SUBMITTED IN PARTIAL FULFILLMENT

OF THE REQUIREMENTS FOR THE

DEGREE OF MASTER OF SCIENCE

at the

MASSACHUSETTS INSTITUTE OF TECHNOLOGY

SEPTEMBER, 1979

(c. June, 1980)

Signature of Author Signature redacted

Department of Electrical Engineering & Computer Science

Approved by Signature redacted

Technical Supervisor, CSDL

Certified by Signature redacted

Thesis Supervisor

Accepted by Signature redacted

Chairman, Departmental Graduate Committee

An Attitude Estimation Algorithm
For a Floated Inertial Reference

by

Stephen G. Sifferlen

Submitted to the Department of Electrical Engineering and Computer Science on October 10, 1979 in partial fulfillment of the requirements for the Degree of Master of Science.

Abstract

This thesis develops an algorithm to estimate the attitude of an inertial navigation system, FLIMBAL, a floated inertial reference. The development is based on the application of optimal linear estimation to a linearized system model. Emphasis is placed on computational efficiency. Its performance is analyzed in detail, including simulation. A procedure for determining an initial nominal attitude for the main linear algorithm is developed. Extensions of the algorithm to include estimation of system parameters with anticipated uncertainty are also presented.

Thesis Supervisor: Gunter Stein,
Adjunct Professor of Electrical Engineering

Acknowledgements

I would like to express my appreciation to Dr. James Negro for his invaluable guidance and assistance, and to Prof. Gunter Stein for his advise and criticism in supervising this thesis. Also, the helpful discussions with Dr. John Dowdle were much appreciated. I would like to thank the Draper 15G staff for the extensive support I received as a Draper Fellow. I would also like to thank Beverly Giarrusso for her cooperation and fine typing of this thesis.

This report was prepared at the Charles Stark Draper Laboratory, Inc. under Contract F04704-78-C-0002 with the Space and Missles Systems Organization of the Air Force Systems Command.

Table of Contents

Chapter

Appendices

List of Figures

List of Tables

I Introduction

A FLIMBAL (Floated Inertial Measurement Ball) [1] is an inertial reference system in which the inertial platform is a ball floated in a fluid and contained in a close-fitting spherical case (Figure 1). The main advantage of this design over a gimbal suspension is improved isolation of the inertial platform from its environment. However, a problem arises in determining the attitude of the inertial reference relative to the vehicle-fixed case since conventional gimbal mounted resolvers are not present.

One technique for reading the attitude of the inertial platform is the Magnetostrictive Attitude Reference System (MARS) which is currently under development. This technique is based on determining geodesic distances on the case between points whose locations are known on the inertial platform (drivers) and points whose locations are known on the case (receivers). These distances are determined by measuring pulsed acoustic wave propagation times between the drivers and receivers. A set of these measurements is taken so that it is unique to the platform attitude, thus enabling unambiguous determination of the attitude from this set.

The algorithm that estimates the platform attitude from the set of measurements is the concern of this thesis.

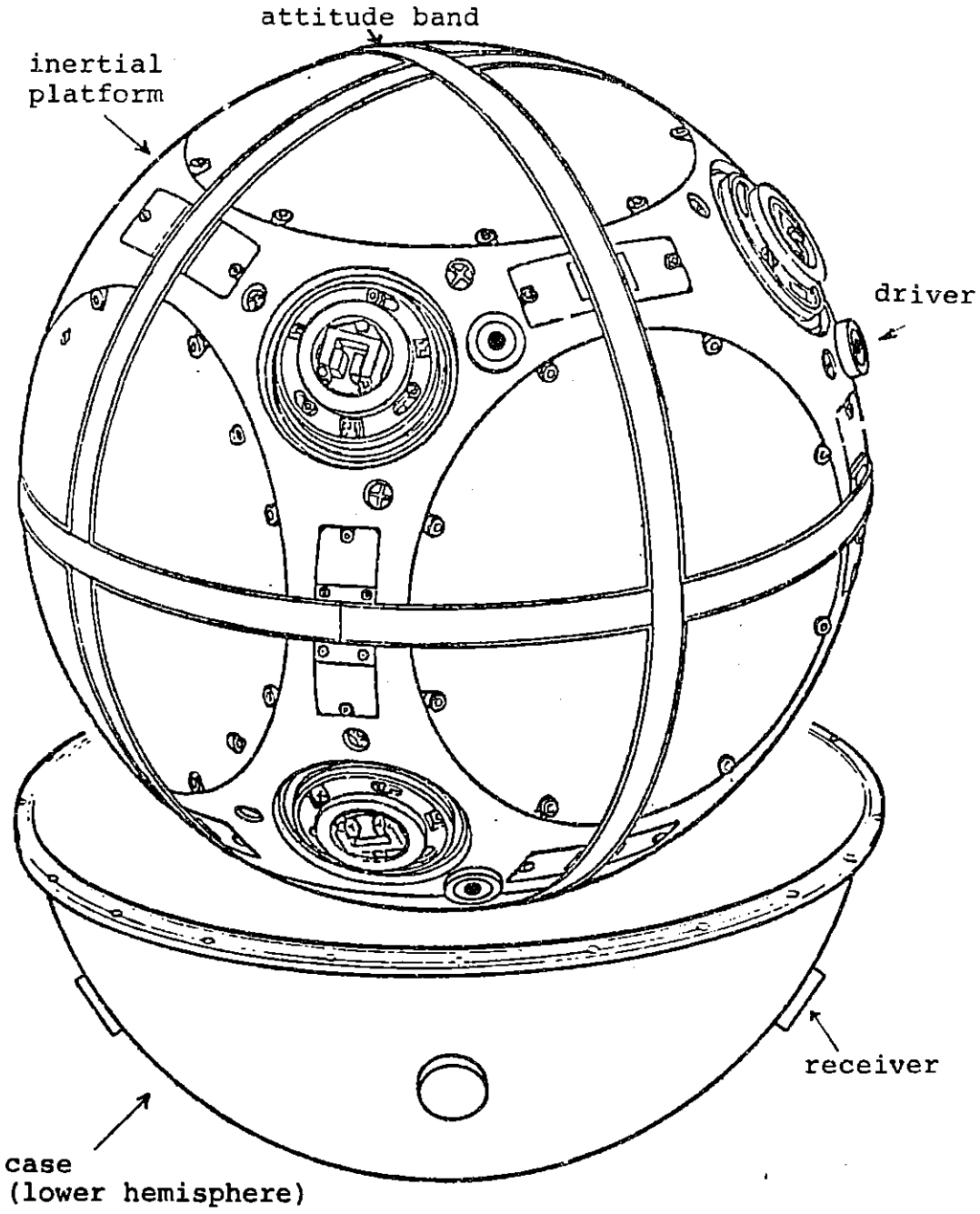

Figure 1.1 FLIMBAL

This problem has been previously addressed by Gail Bonda [3]. She applied an optimal approach and her results surpassed the system specifications. However, her algorithm required excessive computation for implementation in an airborne computer. Thus, a prime motivation in this algorithm development is a reduction of the computation requirements.

1.1 MARS

The MARS system was proposed as an eventual replacement for the current attitude determining system. Currently, attitude, as described by a direction cosine matrix, is determined by sensing the angles between three mutually orthogonal driver bands (which are on the inertial platform) and a receiver band (which is on the case). This technique requires an expensive precision alignment of these bands which must be removed to allow access in the inertial platform. MARS avoids the realignment problems as it uses small drivers on the ball (inertial platform) which do not interfere with access in the ball.

The MARS system has eight magnetostrictive drivers mounted on the ball and four magnetostrictive receivers mounted on the case. The eight drivers are arrayed symmetrically as on the corners of a cube inscribed in

the ball as shown in Figure 1.2.The four receivers are limited to one hemisphere to avoid interference with other subsystems. The receiver's hemisphere is further reduced in size by an equatorial band which attenuates acoustic wave reflections off the seam where the two hemispheres are joined. The locations of the receivers are shown in Figure 1.3. The equatorial band is just narrow enough so that there will always be at least two drivers in the receiver's hemisphere; two drivers are the minimum necessary to determine attitude (Knowing only the position of one driver leaves indeterminate any rotation about an axis determined by that position).

The magnetostrictive property of the nickel case (i.e., nickel contracts in a magnetic field) is used to determine the geodesic distance between a driver and a receiver. A driver modulates a magnetic field which excites a pulsed acoustic wave in the case directly above it. This pulse propagates radially from the point of excitation in a geodesic manner due to the isotropic velocity structure of the case. The pulse is detected by a magnetostrictive receiver mounted on the case as shown in Figure 1.4. The propagation time of the pulse is measured. Then the geodesic distance on the case between the driver and receiver is equal to the measured time multiplied by the acoustic wave group velocity.

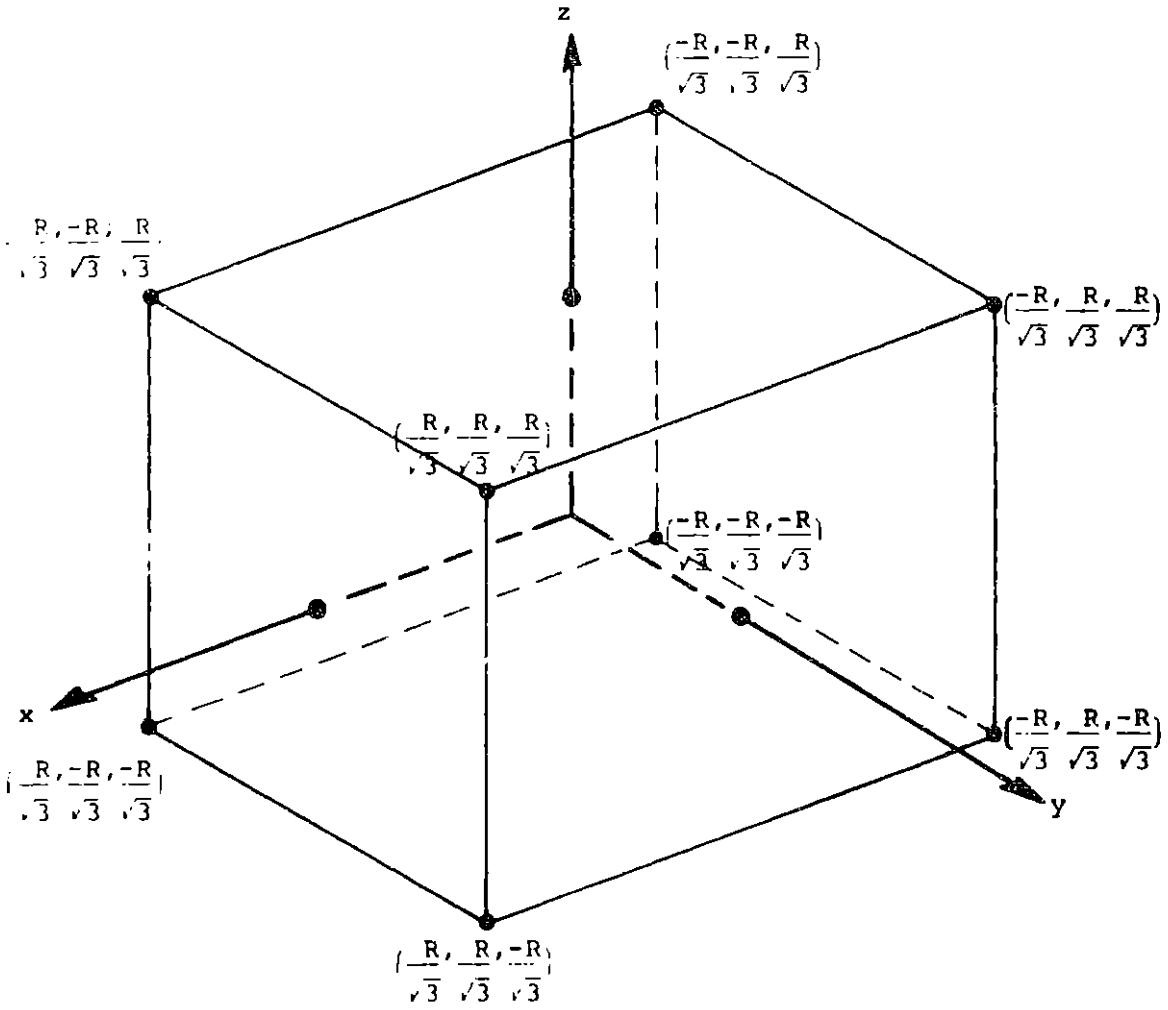

Figure 1.2 Driver Configuration

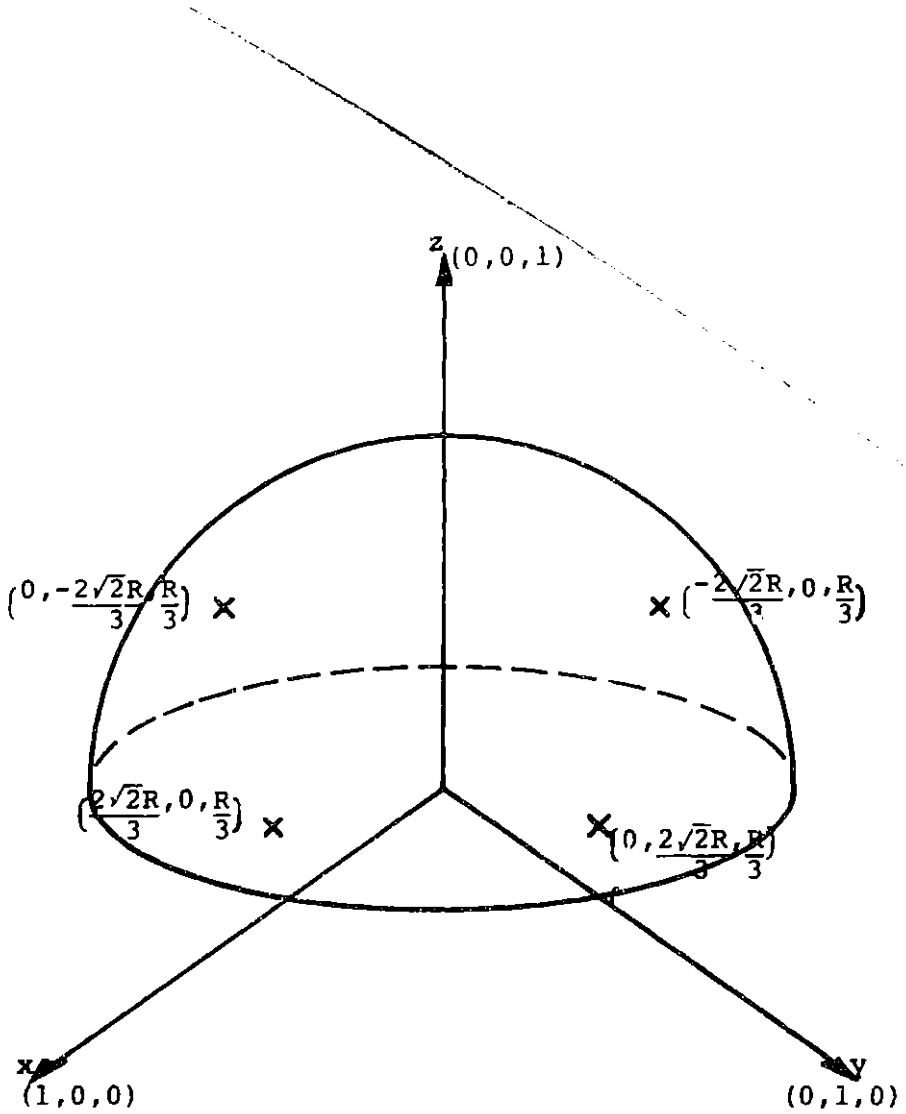

Figure 1.3 Receiver Configuration

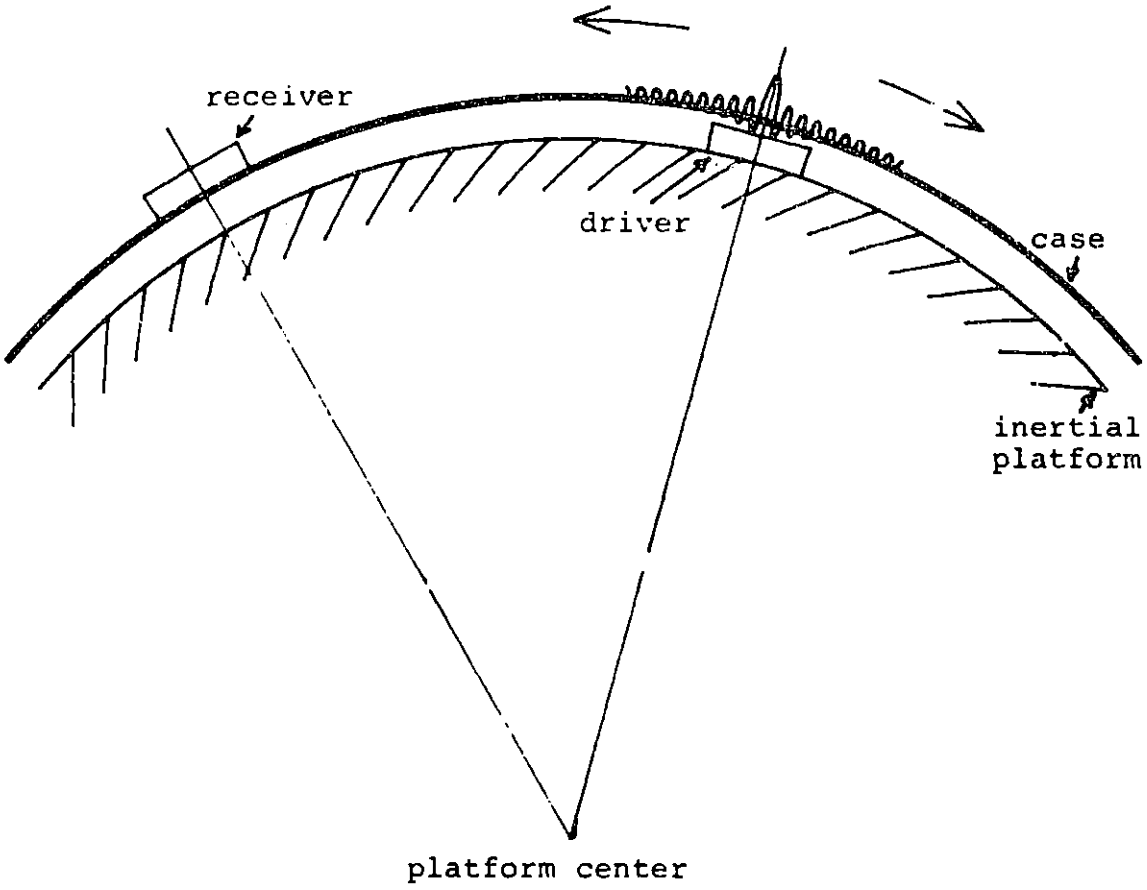

Figure 1.4 Measurement of Pulse Propagation Time

Eight time measurements are taken, each corresponding to a combination of the four receivers and the two drivers which are guaranteed to be in the receiver's hemisphere. Since three measurements are sufficient to determine a driver's position and the platform attitude is determined by two drivers, only six measurements are required and the eight measurements are sufficient.

That only three measurements from a driver are enough to determine its position can be seen by recognizing a measurement as a constraint that the driver lie on a circle centered at the receiver of a radius equal to the distance determined from the measurement. The intersections of two such circles leaves an ambiguity which is resolved by a third measurement (Figure 1.5).

1.2 Thesis Objective

The problem addressed in this thesis is the design of an algorithm to estimate the attitude of an inertial platform as represented by a direction cosine matrix (DCM). The input to the algorithm is the set of measured acoustic pulse propagation times. A major objective in the algorithm design is computational simplicity. Thus, the estimation is formulated using only the present set of measurements. Since, as will be shown, this has met the system specifications (Appendix A) the computational expense of incorporating the system dynamics into the

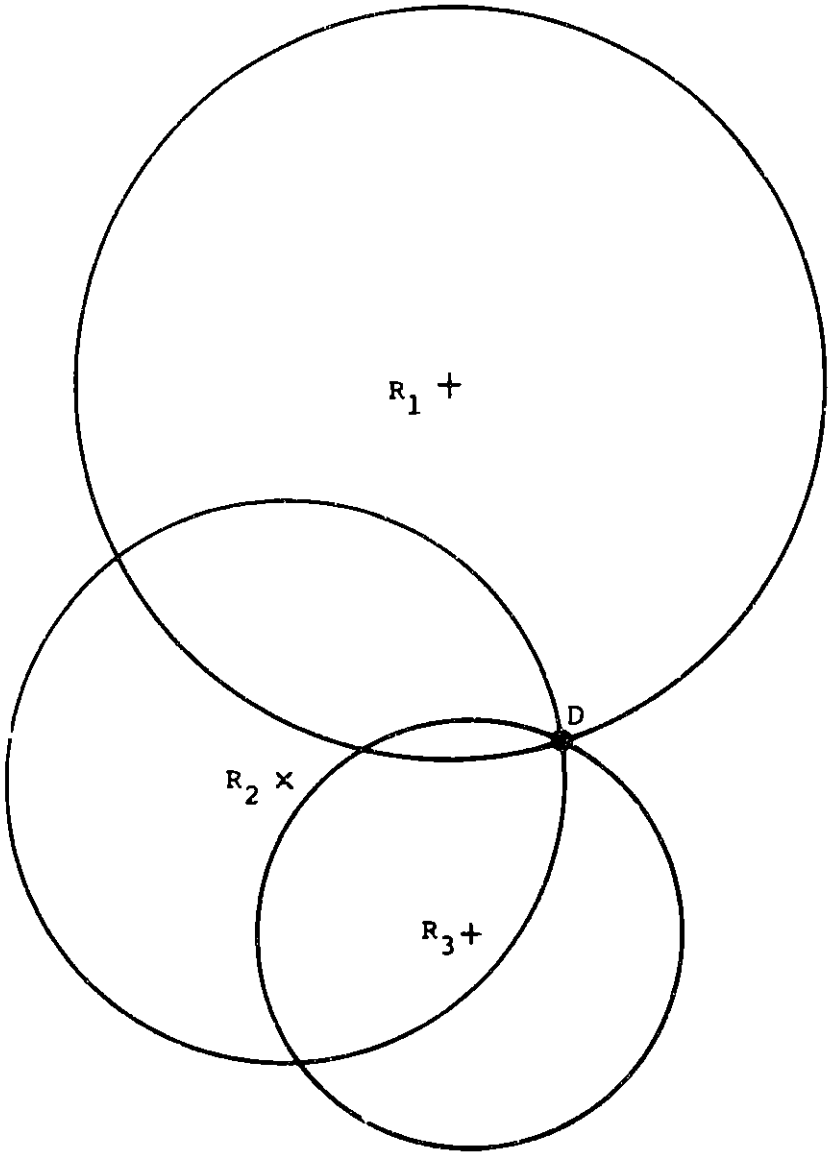

D: Driver
R_1, R_2, R_3: Receivers

Figure 1.5 Driver Position Determination On the Case

estimation for optimal mixing of past measurements is avoided.

Estimation of a DCM is complicated by the six non-linear constraints of a unitary matrix that its nine parameters must satisfy. The approach of this thesis is a linearization of the constraints which is accomplished by representing the estimated DCM by the product of an incremental DCM and a nominal DCM. The incremental DCM is approximated by a matrix containing three unconstrained parameters. The rest of the formulation is linearized and the problem becomes one of unconstrained linear estimation of three parameters.

This thesis develops and evaluates an estimation algorithm based on the above approach. Its performance is characterized by analyses of noise sensitivity and linearization errors. These results are compared to a Monte Carlo simulation. As this is a tracking algorithm, it requires an initialization procedure and so one is designed.

Errors in the modeled system parameters are assumed to be negligible after a calibration procedure. However, some system parameters will still have some anticipated uncertainty, and thus extensions to the basic algorithm are developed to include the uncertain parameters in the estimation.

II Algorithm Development

This chapter discusses the development of the attitude estimation algorithm. The attitude is represented by a direction cosine matrix (DCM) which is estimated from a set of pulse propagation time measurements.

The basis of any estimation algorithm is a model relating the unknown quantities to those quantities which can be measured; in this case, these are the DCM and the pulse propagation times respectively. In the next section, a model for the pulse propagation times is developed. The most efficient estimation techniques are based on linear models. Thus, the model of Section 2.1 is linearized and the resulting increment in attitude is estimated by minimum mean square estimation. An efficient method of updating the nominal attitude by the estimated incremental attitude is selected in Section 2.4. These results are presented as an algorithm in Section 2.5. In the last section, the basic algorithm of Section 2.5 is modified to produce a more efficient suboptimal algorithm.

2.1 Pulse Propagation Time Model

Estimation of the platform attitude is based on the model of the pulsed acoustic wave propagation time as developed below.

Let $\underline{d}^b$, $\underline{d}^i$, $\underline{r}^b$ be unit vectors locating drivers in the body-fixed (case fixed) and in-

ertial(ball fixed)frames and a receiver in the inertial frame respectively.

t be the measured pulse propagation time from driver to receiver.

V be the isotropic acoustic velocity in the case.

R be the radius of the case.

θ be the angle between $\underline{d}^b$ and $\underline{r}^b$.

a be the geodesic arc length on the case between the driver and receiver.

These definitions are illustrated in figure 2.1

Then

$$t = \frac{a}{V} = \frac{R\theta}{V} \qquad 2.1.1$$

Since the dot product of two unit vectors is the cosine of the angle between them

$$\theta = \cos^{-1}(\underline{r}^b \cdot \underline{d}^b) \qquad 2.1.2$$

where Θ is taken at its principle valve.

Let C_i^b be the DCM transformation from the inertial frame to the body fixed frame. Then

$$\underline{d}^b = C_i^b \, \underline{d}^i \qquad 2.1.3$$

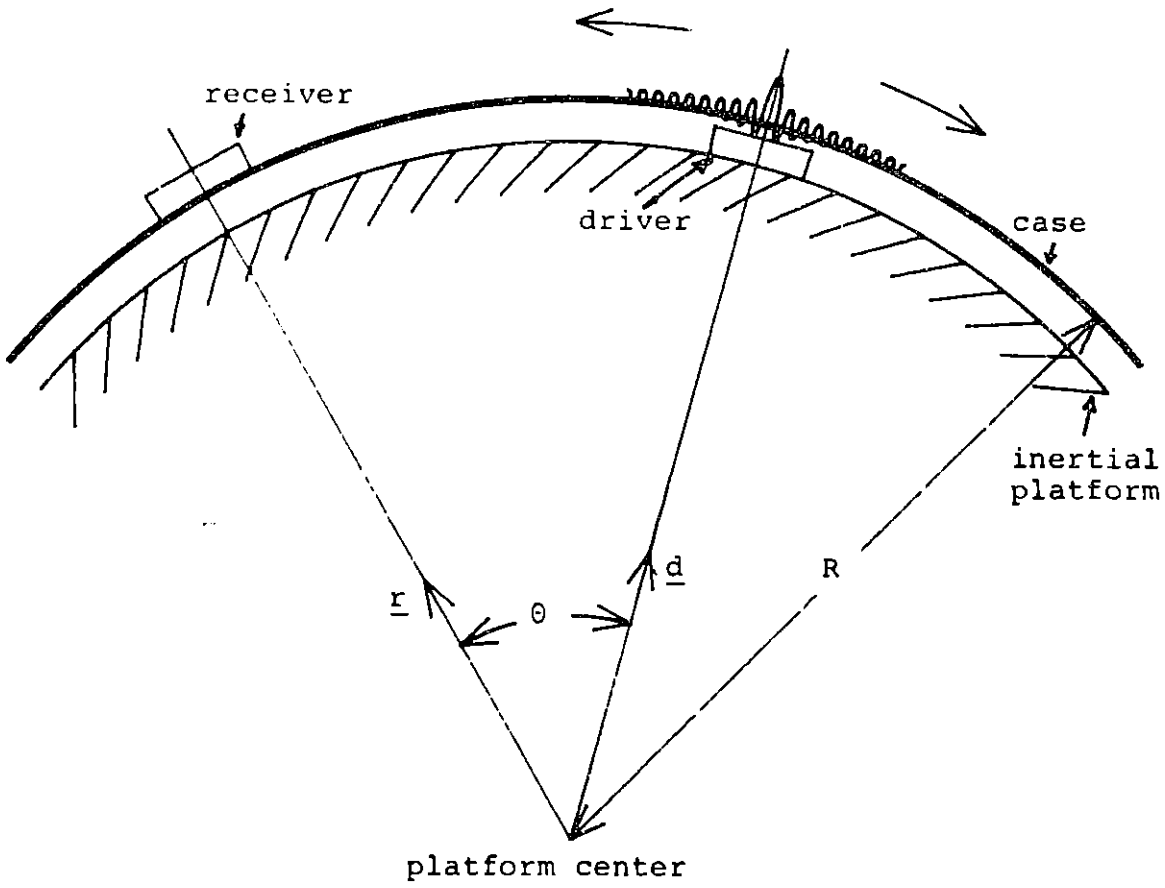

Figure 2.1 Time Measurement Geometry

Combining equation 2.1.1, 2.1.2 and 2.1.3 gives the model for the pulse propagation time

$$t = \frac{R}{V} \cos^{-1}\left(\underline{r}^b \cdot C_i^b \, \underline{d}^i\right) \qquad 2.1.4$$

For this application the variables in equation 2.1.4 are t and C_i^b while R, V, $\underline{r}^b$ and $\underline{d}^i$ are known constants which are assumed to have been accurately calibrated.

2.2 Model Linearization

The model of equation 2.1.4 is both nonlinear and nonlinearly constrained by the requirement that a DCM be orthogonal. In order to use the computationally efficient techniques of estimation that apply to linear unconstrained models, this model must by made likewise linear and unconstrained. Our approach will be to first remove the constraints and then linearize the model.

As a preliminary in anticipation of linearization the DCM C_i^b is expressed as

$$C_i^b = C_{b'}^b \, C_i^{b'} \qquad 2.2.1$$

where $C_i^{b'}$ is a DCM representing a known nominal attitude and $C_{b'}^b$ is a DCM representing the small angle rotation between the nominal and actual attitudes. The approach

will be to estimate $C_{b'}^{b}$ and use it to update

$$\hat{C}_i^b = \hat{C}_{b'}^{b}\, C_i^{b'} \qquad 2.2.2$$

The six constraints on the nine parameters of $C_{b'}^{b}$ are avoided by expressing $C_{b'}^{b}$ in terms of three unconstrained parameters. If the three parameters are arranged in a vector $\underline{\mu}$ then $C_{b'}^{b}$ may be expressed a (see Appendix B)

$$C_{b'}^{b} = \sum_{k=0}^{\infty} \frac{M^k}{k!} \qquad 2.2.3$$

where M^0 is the identity matrix I and

$$M \triangleq \begin{bmatrix} 0 & -\mu_z & \mu_y \\ \mu_z & 0 & -\mu_x \\ -\mu_y & \mu_x & 0 \end{bmatrix} \qquad 2.2.4$$

$\underline{\mu}$ has an interpretation similar to that of a quaternion description. The direction of $\underline{\mu}$ is the axis of the rotatation of $C_{b'}^{b}$, and the angle rotated is given by the magnitude of $\underline{\mu}$.

Applying equations 2.2.1 and 2.2.3 to 2.1.4 gives the unconstrained model relating the pulse propagation times t to the incremental attitude $\underline{\mu}$

$$t = \frac{R}{V} \cos^{-1} \left[\underline{r}^b \cdot \left(\sum_{k=0}^{\infty} \frac{M^k}{k!} \right) C_i^{b'} \underline{d}^i \right] \qquad 2.2.5$$

Now the model will be linearized. A convenient nominal attitude $C_i^{b'}$ about which to linearize the unconstrained model is the attitude estimated from the previous set of measurements. As the platform rotation between measurements is small, i.e. less than 20 milliradians, error due to linearization about the previous attitude estimate will also be small.

First $C_{b'}^{b}$ is linearized in the elements of $\underline{\mu}$ by truncating the series of equation 2.2.3 after the first order term

$$C_{b'}^{b} = I + M \qquad 2.2.6$$

This form of $C_{b'}^{b}$ is also a linearization of the constraint that a DCM be orthogonal. It satisfies that constraint to the first order

$$C_{b'}^{b}\, C_{b'}^{b^T} = (I + M)\,(I + M)^T \qquad 2.2.7$$

$$= (I + M)\,(I - M) \qquad 2.2.8$$

$$= I - M^2 \qquad 2.2.9$$

and M^2 contains only second order terms.

Defining

$$\underline{d}^{b'} \triangleq C_i^{b'} \underline{d}^i \qquad 2.2.10$$

the model becomes

$$t = \frac{R}{V} \cos^{-1} \left(\underline{r}^b \cdot (I+M)\, \underline{d}^{b'} \right) \qquad 2.2.11$$

Then the inverse cosine is linearized about the nominal attitude which is represented by $C_{b'}^{b} = I$

$$t = \frac{R}{V} \cos^{-1} \left(\underline{r}^b \cdot \underline{d}^{b'} \right)$$

$$- \frac{R}{V} \left(1 - \left(\underline{r}^b \cdot \underline{d}^{b'} \right)^2 \right)^{-1/2} \left(\underline{r}^b \cdot M\underline{d}^{b'} \right)$$

2.2.12

The first term on the right hand side of 2.2.12 is the model of equation 2.1.4 applied to the nominal attitude.

Thus a nominal pulse propagation time t' is defined as

$$t' = \frac{R}{V} \cos^{-1} \left(\underline{r}^b . \underline{d}^{b'} \right) \qquad 2.2.13$$

and the model becomes

$$\Delta t = t - t' = - \frac{R}{V} \left(1 - \underline{r}^b . \underline{d}^{b'} \right)^2 \right)^{-1/2} \left(\underline{r}^b . M \underline{d}^{b'} \right)$$

2.2.14

Here it is useful to note that the skew symmetric form of the matrix M has the property, such that for a vector v expressed in the b frame

$$M \underline{v} = \underline{\mu} \times \underline{v} \qquad 2.2.15$$

where ' x ' denotes a cross product. Thus

$$\underline{r}^b . M \underline{d}^{b'} = \underline{r}^b . \left(\underline{\mu} \times \underline{d}^{b'} \right) \qquad 2.2.16$$

The triple vector product is rearranged

$$\underline{r}^b . \underline{\mu} \times \underline{d}^{b'} = \left(d^{b'} \times r^b \right) . \underline{\mu} \qquad 2.2.17$$

This model is further simplified by noting that

$$|\underline{d}^{b'} \times \underline{r}^{b}| = \sin\theta \qquad 2.2.18$$

and

$$\underline{d}^{b'} \cdot \underline{r}^{b} = \cos\theta \qquad 2.2.19$$

where θ is the angle between $\underline{d}^{b'}$ and $\underline{r}^{b}$ at the nominal attitude when the b and b' frames coincide. Then

$$\left(1 - (\underline{r}^{b} \cdot \underline{d}^{b'})^2\right)^{-1/2} = \left(1 - \cos^2\theta\right)^{-1/2} \qquad 2.2.20$$

$$= \left(\sin\theta\right)^{-1} \qquad 2.2.21$$

$$= |\underline{d}^{b'} \times \underline{r}^{b}|^{-1} \qquad 2.2.22$$

Applying equations 2.2.16, 2.2.17 and 2.2.22 to equation 2.2.14 gives the linearized unconstrianed model:

$$\Delta t = -\frac{R}{V} \frac{\underline{d}^{b'} \times \underline{r}^{b}}{|d^{b'} \times \underline{r}^{b}|} \cdot \underline{\mu} \qquad 2.2.23$$

This model has a simple geometric interpretation. To the first order only a rotation in the plane defined by $\underline{r}$ and $\underline{d}$ will affect a time measurement between $\underline{r}$ and $\underline{d}$. A rotation in the plane defined by $\underline{r}$ and $\underline{d}$ has a principle axis $\underline{g}$ where $\underline{g}$ is a unit vector normal to the plane. Before the rotation, $\underline{g}$ is given by

$$\underline{g} = \frac{\underline{r}^b \times \underline{d}^{b'}}{|r^b \times d^{b'}|} \qquad 2.2.24$$

The angle θ_g of rotation in the plane of $\underline{r}$ and $\underline{d}$ from a rotation $\underline{\mu}$ is given by

$$\theta_g = \underline{g} \cdot \underline{\mu} \qquad 2.2.25$$

From equation 2.1.1 the time difference Δt in a measurement due to a rotation by θ_g is

$$\Delta t = \frac{R}{V} \theta_g \qquad 2.2.26$$

combining equations gives the linear unconstrained model

$$\Delta t = \frac{R}{V} \frac{\underline{r}^b \times \underline{d}^{b'}}{|\underline{r}^b \times \underline{d}^{b'}|} \cdot \mu \qquad 2.2.27$$

To apply this result to the eight measurements we will need the following definitions:

t_{ij} is the measured pulse propagation time between driver i and receiver j.

$\underline{d}_i^i$ is the position unit vector of the i^{th} driver in the inertial frame.

$\underline{r}_j^b$ is the position unit vector of the j^{th} receiver in the body fixed frame.

t'_{ij} is the nominal pulse propagation time between driver i and receiver j.

$$\Delta t_{ij} = t_{ij} - t'_{ij}$$

Then the model is

$$\Delta t_{ij} = \frac{R}{V} \frac{\underline{r}_j^b \times \underline{d}_i^{b'}}{|\underline{d}_i^{b'} \times \underline{r}_j^b|} \cdot \underline{\mu} \qquad 2.2.28$$

Forming equation 2.2.28 for all combinations of drivers and receivers gives a set of eight linear equations, which may be conveniently expressed as the linear vector equation:

$$\Delta \underline{t} = B \underline{\mu} \qquad 2.2.29$$

where

$$\Delta \underline{t} = \begin{bmatrix} \Delta t_{11} \\ \Delta t_{12} \\ \vdots \\ \Delta t_{24} \end{bmatrix} \qquad 2.2.30$$

$$B = \frac{R}{V} \begin{bmatrix} \dfrac{\underline{r}_1^b \times \underline{d}_1^{b'}}{|\underline{d}_1^{b'} \times \underline{r}_1^b|} \\ \vdots \\ \dfrac{\underline{r}_4^b \times \underline{d}_2^{b'}}{|\underline{d}_2^{b'} \times \underline{r}_4^b|} \end{bmatrix} \qquad 2.2.31$$

each vector represents a row

2.3 Estimation

In reality additive noise corrupts the measurements. This is due to random errors in the pulse detector, and to small deviations from the nominal in the case acoustic velocity. The approach taken here is to estimate $\underline{\mu}$ from the noisy $\underline{\Delta t}$ using a Moore-Penrose pseudoinverse B^{+}[8], to invert the relation of equation 2.2.29. The estimate $\hat{\underline{\mu}}$ of $\underline{\mu}$ is

$$\hat{\underline{\mu}} = \left(B^{T}B\right)^{-1}B^{T}\,\underline{\Delta t} \qquad 2.3.1$$

$$= B^{+}\,\underline{\Delta t}$$

and the estimate of $\underline{\Delta t}$ is defined as 2.3.2

$$\hat{\underline{\Delta t}} = B\,\hat{\underline{\mu}} \qquad 2.3.3$$

This pseudoinverse will always exist as for the proposed system configuration the matrix B has a rank of 3. This estimator has the desirable property of minimizing the root of the sum of the squared errors in $\hat{\underline{\Delta t}}$; it minimizes $|\underline{\Delta t} - \hat{\underline{\Delta t}}|$.

For this application the pseudoinverse can also be said to be an optimal linear estimator in the Bayesian sense of minimizing $E|\underline{\mu} - \hat{\underline{\mu}}|$ where E denotes expectation. This approach requires characterizations of the second order statistics for $\underline{\mu}$, a priori, and for the noise. The

noise sources can be reasonably modeled as additive, independent, zero mean and equal variance. Thus if $\underline{n}$ denotes the random noise vector and Q is its correlation matrix then

$$Q = E\ (nn^T) = \sigma_n^2 I \qquad 2.3.4$$

where σ_n^2 is the variance of the measurement noise.

Let P_o be the á priori covariance matrix for $\underline{\mu}$. Then the optimal linear estimate of $\underline{\mu}$ is [5]

$$\hat{\underline{\mu}} = (B^T Q^{-1} B + P_o^{-1})^{-1}\ B^T Q^{-1}\ \underline{\Delta t} \qquad 2.3.5$$

Applying equation 2.3.4 to equation 2.3.5

$$\hat{\underline{\mu}} = (B^T B + \sigma_n^2\ P_o^{-1})^{-1}\ B^T\ \underline{\Delta t} \qquad 2.3.6$$

As there is no á priori information on $\underline{\mu}$ in this formulation, $\underline{\mu}$ may be considered to have an extremely large á priori covariance. Thus $\sigma_n^2\ P_o^{-1}$ is very small compared to $B^T B$ and the optimal linear estimator becomes the pseudoinverse, B^+

$$\hat{\underline{\mu}} = (B^T B)^{-1}\ B^T\ \underline{\Delta t} \qquad 2.3.6$$

2.4 Updating the Nominal Attitude

The estimate $\hat{C}_i^b$ of C_i^b is computed from

$$\hat{C}_i^b = \hat{C}_{b'}^b \; C_i^{b'} \qquad 2.4.1$$

where $\hat{C}_{b'}^b$ is computed from $\hat{\underline{\mu}}$. In order to reduce computational load an approximate form of $C_{b'}^b$ could be used. Use of an approximate $C_{b'}^b$ will leave $\hat{C}_i^b$ non orthogonal, and will periodically require reorthogonalization.

This section presents forms of $\hat{C}_{b'}^b$ and orthogonalization procedures, and choses the most computationally efficient combination.

$\hat{C}_{b'}^b$ is expressed exactly by equation 2.2.3. Easier to calculate is the following equation from Appendix B which is based on a four parameter attitude representation.

$$\hat{\alpha} = |\hat{\mu}| \qquad 2.4.2$$

$$\hat{\underline{\nu}} = \hat{\mu}/\hat{\alpha} \qquad 2.4.3$$

$$\hat{C}_{b'}^b = I + \sin\alpha \; N + (1-\cos\alpha)N^2 \qquad 2.4.4$$

In the interest of reducing computation a low order update matrix may be formed directly from $\hat{\underline{\mu}}$. The first order update matrix is obtained by truncating the series of equation 2.2.8 to first order terms

$$\hat{C}_b^b = I + M \qquad 2.4.5$$

Similarly the second order update matrix is

$$\hat{C}_b^b = I + M + \tfrac{1}{2} M^2 \qquad 2.4.6$$

After being updated by an approximate C_b^b, the new estimate $\hat{C}_i^b$ is no longer an orthogonal matrix. To achieve accuracy it is necessary to periodically orthogonalize $\hat{C}_i^b$. Once a $\hat{C}_i^b$ is orthogonalized it is used as the nominal matrix for the next estimate. Then the next estimate will contain error due to only one update, and orthogonalization effectively clears the accumulated error due to an approximate update.

A straight forward orthogonalization routine is the Gran-Schmidt procedure [9]. The procedure is described in the following.

Let C be a 3 x 3 matrix

C^N be C after normalization by the Gran-Schmidt procedure

$\tilde{C}$ be a temporary matrix used in the computation

C, C^N and $\tilde{C}$ are partitioned into their three column vectors e.g.

$$C = \begin{bmatrix} C_1 & C_2 & C_3 \end{bmatrix} \qquad 2.4.7$$

Then

$$C_1^N = C_1 / |C_1| \qquad 2.4.8$$

$$\tilde{C}_2 = C_2 - (C_1^N \cdot C_2) C_1^N \qquad 2.4.9$$

$$C_2^N = \tilde{C}_2 / |\tilde{C}_2| \qquad 2.4.10$$

$$\tilde{C}_3 = C_3 - (C_1^N \cdot C_3) C_1^N - (C_2^N - C_3) C_2^N \qquad 2.4.11$$

$$C_3^N = \tilde{C}_3 / |\tilde{C}_3| . \qquad 2.4.12$$

C_1 is normalized to form C_1^N. Any component of C_1^N in C_2 is removed so that $\tilde{C}_2$ is orthogonal to C_1^N. Then $\tilde{C}_2$ is

normalized to form C_2^N. Any components of C_1^N and C_2^N in C_3 are removed so that $\tilde{C}_3$ is orthogonal to both C_1^N and C_2^N. Then $\tilde{C}_3$ is normalized to form C_3^N. Thus C^N is composed of mutually orthogonal unit vectors.

That is, since

$$C^N = \left[\underline{C}_1^N \quad \underline{C}_2^N \quad C_3^N\right] \tag{2.4.13}$$

then

$$C^{N^T} C^N = \begin{bmatrix} \underline{C}_1^{N^T} \\ \underline{C}_2^{N^T} \\ \underline{C}_3^{N^T} \end{bmatrix} [\underline{C}_1^N \; \underline{C}_2^N \; \underline{C}_3^N] \tag{2.4.14}$$

$$= \begin{bmatrix} \underline{C}_1^{N^T} \underline{C}_1^N & \underline{C}_1^{N^T} \underline{C}_2^N & \underline{C}_1^{N^T} \underline{C}_3^N \\ \underline{C}_2^{N^T} \underline{C}_1^N & \underline{C}_2^{N^T} \underline{C}_2^N & \underline{C}_2^{N^T} \underline{C}_3^N \\ \underline{C}_3^{N^T} \underline{C}_1^N & \underline{C}_3^{N^T} \underline{C}_2^N & \underline{C}_3^{N^T} \underline{C}_3^N \end{bmatrix} \tag{2.4.15}$$

$$= \begin{bmatrix} 1 & 0 & 0 \\ 0 & 1 & 0 \\ 0 & 0 & 1 \end{bmatrix} = I \tag{2.4.16}$$

And thus C^N satisfies the constraint on an orthogonal matrix.

With the goal of improving accuracy, and achieving greater efficiency another orthogonalization technique, the 'best fit' method was investigated. The best fit method finds an orthogonal matrix C^N, such that the three angles between a column C_j of C and its corresponding column C_j^N of C^N are approximately minimized in a least sum of squares sense. This approximation becomes more exact as C becomes more orthogonal. This method acheives the minimization by distributing the corrections to the non-perpendicularity of pairs evenly. For example if C_1 and C_2 were not orthogonal by an angle of α, C_1 and C_2 would each be rotated by an angle of $\alpha/2$. In the following description of the best fit method C' and C" are temporary matrices used in computation, and their subscripts denote columns. First half of the projection of C_2 and C_3 or C_1 are removed from C_1 which is normalized to form C_1^N

$$C_1' = C_1 - 1/2\ (C_2 \cdot C_1)\ C_2 - 1/2\ (C_3 \cdot C_1)\ C_3 \qquad 2.4.17$$

$$C_1^N = C_1'/|C_1'| \qquad 2.4.18$$

Then the remaining components of C_2 that are shared with C_1^N are removed from C_2

$$C_2'' = C_2 - (C_1^N \cdot C_2)C_1^N \qquad 2.4.19$$

Similarly with C_3

$$C_3'' = C_3 - (C_1^N \cdot C_3)C_1^N \qquad 2.4.20$$

Now C_1^N is perpendicular to the plane of C_2'' and C_3'', and the rest of the procedure involves making C_2'' and C_3'' orthogonal. Half the projection of C_2'' on to C_3'' is removed from C_2''

$$C_2' = C_2'' - 1/2\ (C_3'' \cdot C_2'')C_3'' \qquad 2.4.21$$

and

$$C_2^N = C_2'/|C_2'| \qquad 2.4.22$$

Then the remaining component of C_2^N in C_3'' is removed from C_3''

$$C_3' = C_3'' - (C_3'' \cdot C_2^N)C_2^N \qquad 2.4.23$$

$$C_3^N = C_3'/|C_3'| \qquad 2.4.25$$

A form of $\hat{C}^b_{b'}$ and an orthogonalization procedure will be chosen from the above based on its computational efficiency. Here computational efficiency is the ability to provide a level of accuracy with a minimum of computation. The computation requirements of the above algorithms are shown in Table 2.1.

The best fit orthogonalization procedure requires nearly twice the computation of the Gram-Schmidt procedure. However, when simulated it provided a negligible increase in accuracy, which was due primarily to the small angles involved. Thus for this case the Gram-Schmidt procedure is the more efficient.

In order to chose among the forms of $\hat{C}^b_{b'}$ their accuracies are determined. First note that the exact form of equation 2.4. is orthogonal, and has no corresponding error. As defined in Appendix A the error $C^b_{b'}$ associated with the use of an approximate $\hat{C}^b_{b'}$ is the maximum singular value of the error matrix $E^b_{b'}$ where

$$E^b_{b'} = C^b_{b'} - \hat{C}^b_{b'} \qquad 2.4.26$$

$E^b_{b'}$ has been computed in Appendix C for the first, and second order update matrices. The maximum error from the use of a first order update

Table 1

Computation Requirements for Update Procedures

	MULTIPLIES	DIVISIONS	ADDS/SUBTRACTS	MISCELLANEOUS
Computation of $C_b^{b'}$				
Exact	45	1	33	square root,cosine
2^{nd} Order	33		30	
1^{st} Order	18		18	
Orthogonalization				
Gram-Schmidt	36	3	21	3 square roots
'Best Fit'	54	3	36	3 square roots

is

$$\varepsilon_b^b = \sqrt{(\sin\alpha - \alpha)^2 + (1 - \cos\alpha)^2} \qquad 2.4.27$$

The maximum error from the use of a second order update is

$$\varepsilon_{b'}^b = \sqrt{(\sin\alpha - \alpha)^2 + (1 - \cos\alpha - \frac{\alpha^2}{2})^2} \qquad 2.4.28$$

The maximum rotation of the platform between measurements is 20 miliradians. For this value of α the first order error is 2.0×10^{-4}, and the second order error is 1.33×10^{-6}. These correspond to angular errors of .2 milliradian and 1.3 μrad for the first and second order algorithm respectively.

An upper bound on the error due to a series of updates in terms of its individual ε is developed.

$$\varepsilon_{b"}^b = \max_{V_{b"}} |(C_b^b, C_{b"}^{b'} - \hat{C}_b^b, \hat{C}_{b"}^b)V^{b"}| \qquad 2.4.29$$

$$= \max_{V^{b"}} |(E_b^b, C_{b"}^{b'} + C_b^b E_{b"}^b - E_b^b E_{b"}^{b'})V^{b"}| \qquad 2.4.30$$

$$\leq \max_{V^{b"}} |E_b^b, C_{b"}^{b'} V^{b"}| + \max |C_b^b, E_{b"}^{b'} V^{b"}| + \max |E_b^b, E_{b"}^{b'} V^{b"}| \qquad 2.4.31$$

Since the matrices $C_{b"}^{b'}$ and $C_{b'}^b$ do not change the magnitude of a vector

$$\varepsilon^{b}_{b''} \leq \varepsilon^{b}_{b'} + \varepsilon^{b}_{b''} + \max_{V^{b'}} | \varepsilon^{b}_{b'} V^{b'} | \max_{V^{b'}} | \varepsilon^{b'}_{b''} V^{b''} | \quad 2.4.32$$

$$\leq \varepsilon^{b}_{b'} + \varepsilon^{b}_{b''} + \varepsilon^{b}_{b'} \varepsilon^{b}_{b''} \quad 2.4.33$$

If the errors are small then the second order term in equation 2.4.33 is negligible and

$$\varepsilon^{b}_{b''} \leq \varepsilon^{b}_{b'} + \varepsilon^{b'}_{b''} \quad 2.4.34$$

Thus to first order a bound on the cumulative error is the sum of the individual bounds. And the error $\varepsilon^{b}(K)$ as a function of the number of updates K is bounded by

$$\varepsilon^{b}(K) \leq (2.0 \times 10^{-4} \text{ radians}) K \quad 2.4.35$$

and for the second order matrix

$$\varepsilon^{b}(K) \leq (1.33 \times 10^{-6} \text{ radians}) K \quad 2.4.36$$

This bound is conservative as it ignores correction of orthogonal errors that just define a new nominal attitudes

It is anticipated that at least 6.0×10^{-4} radians of the total 2.91×10^{-3} radians error budget can be allocated to update error. For this level of performance the first order matrix can be used for 3 updates in between orthogonalizations, and the second order matrix may be used for 450 updates between orthogonalizations. Comparing requirements for multiplies, the average number per update

required for the first order matrix is 18 plus a third that are required for the Gran-Schmidt procedure, 12 giving an average total of 30. The second order matrix requires an average total of 33 multiples as the average contribution of the orthogonalization over 450 updates is negligible. The exact matrix requires 45 multiplies per update. Based on the multiply requirements which are indicative of the overall computation requirements, the exact matrix is the least efficient in meeting the accuracy requirements even though it provides no error. The first and second order are close, but for an update error budget of 6.0×10^{-4} radians or greater the first order matrix is the most efficient for this estimation algorithm.

2.5 The Algorithm

The complete algorithm for estimation of C_i^b is presented in a block diagram in Figure 2.2.This algorithm solves

$$B^T B \, \hat{\underline{\mu}} = B^T \, (\underline{t} - \underline{t}') \qquad 2.5.1$$

by Gaussian elimination. This procedure is more efficient than computing $\hat{\underline{\mu}}$ directly using the matrix inversion of equation 2.3.1. The linearized model B and the nominal pulse propagation times $\underline{t}'$ are computed for the nominal DCM, $C_i^{b'}$. The nominal propagation times $\underline{t}'$ are subtracted from the measured pulse propagation times $\underline{t}$, to give $\underline{\Delta t}$. Then after forming $B^T B$ and $B^T \underline{\Delta t}$ equation 2.5.1

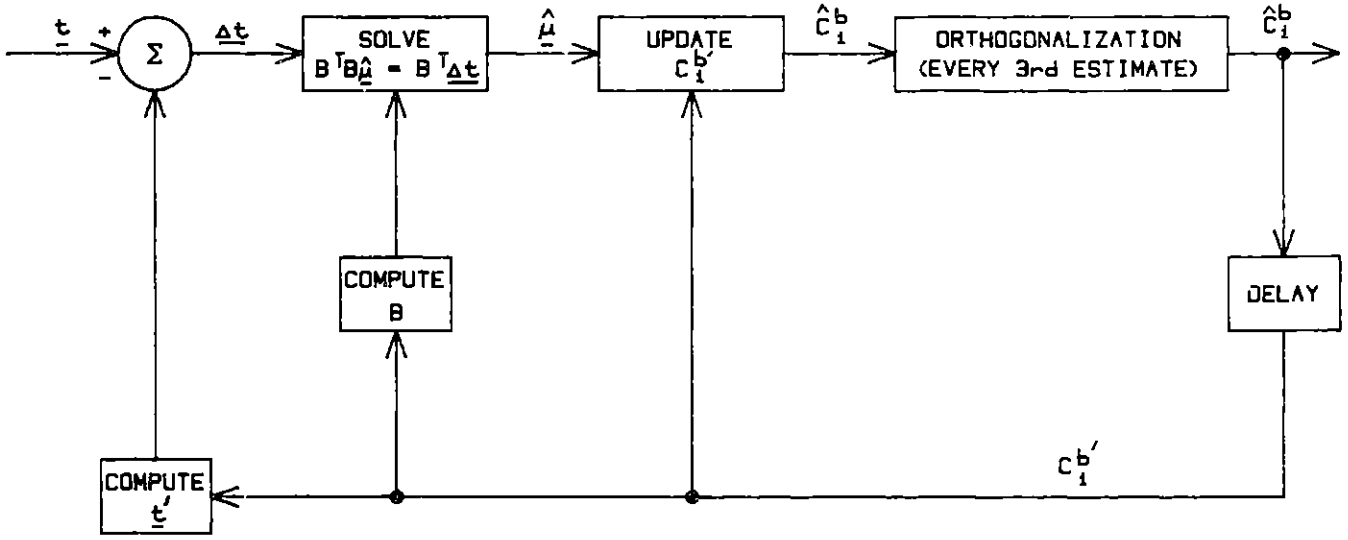

FIGURE 2.2 THE BASIC ATTITUDE ESTIMATION ALGORITHM

is solved to give $\hat{\underline{\mu}}$. $\hat{C}^b_b$, is formed from $\hat{\underline{\mu}}$ as I + M and is efficiently multiplied by $C_i^{b'}$ to get the estimate $\hat{C}^b_i$. Every third iteration $\hat{C}^b_i$ is orthogonalized by the Gram-Schmidt procedure. The estimate matrix is used as the nominal matrix in the next iteration as represented by the delay in Figure 2.2.

As a prime motivation for this thesis is to reduce the computation in the estimation algorithm a preliminary point for evaluation is its computation requirements. These are presented in Table 2.2, the computational requirement of this algorithm is a reduction of an order of magnitude over the previous algorithm [3] ,which had a requirement typified by a multiplication count in excess of 2500 per attitude estimate. This estimated count was obtained by conservatively enumerating the requirements of the components of the numerical method as described in section 4.2 of [3] .

2.6 A Suboptimal Algorithm

To reduce computation, the computation of the basic algorithm was rearranged to produce a less optimal in noise performance, but computationally simpler algorithm. Its development begins with the model at equation 2.1.4.

$$\cos \frac{V}{R} t = r^b \cdot C_i^b \, d^i \qquad 2.6.1$$

Table 2.2
Computational Requirements
for the Basic Algorithm

EQUATION	TIME CALCULATED	MULTIPLIES	DIVISIONS	ADDS/SUBTRACTS	MISCELLANEOUS
2.1.3	2	18		12	
2.2.13	8	32		16	8 $\cos^{-1}$
2.2.31	1	80	8	40	8 square roots
$\underline{t}-\underline{t}'$	1			8	
$B^T B$	1	72		63	
$B^T \underline{\Delta t}$	1	24		21	
Gaussian elimination	1	11	6	11	
2.2.2	1	18		18	
Gram-Schmidt orthogonalization	*	9	1	7	1 square root
TOTAL		264	15	196	9 square roots 8 $\cos^{-1}$

*Averaged over 3 iterations

The left hand side is defined as τ

$$\tau = \cos \frac{V}{R} t \qquad 2.6.2$$

C_i^b is approximated by a product of an incremental, and nominal matrix as in equation 2.2.11,

$$\tau = \underline{r}^b \cdot (I + M)\, C_i^{b'}\, \underline{d}^i \qquad 2.6.3$$

$$= \underline{r}^b \cdot \underline{d}^{b'} + \underline{r}^b \cdot M\underline{d}^{b'} \qquad 2.6.4$$

where $\underline{d}^{b'} = C_i^{b'}\, \underline{d}^i$.

The first term of the right hand side is τ evaluated at the attitude represented by the nominal DCM. Thus a nominal τ, τ' can be defined as

$$\tau' = \cos \frac{V}{R} t' = \underline{r}^b \cdot \underline{d}^{b'} \qquad 2.6.5$$

Substituting equation 2.6.5 in equation 2.6.4, and defining a $\Delta\tau$

$$\Delta\tau' = \tau - \tau' = \underline{r}^b \cdot M\, \underline{d}^{b'} \qquad 2.6.6$$

Applying equations 2.2.16 and 2.2.17

$$\Delta\tau = (\underline{d}^{b'} \times \underline{r}^b) \cdot \underline{\mu} \qquad 2.6.7$$

Utilizing the conventions established previously, and applying equation 2.6.7 to the eight measurements produces a system of linear equations which is conveniently expressed in a linear vector equation

$$\underline{\Delta\tau} = \beta\underline{\mu} \qquad 2.6.8$$

where $\underline{\Delta\tau} = \begin{bmatrix} \cos \frac{V}{R} t_{11} - \cos \frac{V}{R} t'_{11} \\ \vdots \\ \cos \frac{V}{R} t_{24} - \cos \frac{V}{R} t'_{24} \end{bmatrix}$ 2.6.9

and

$$\beta = \begin{bmatrix} d_1^{b'} \times r_1^b \\ \vdots \\ d_2^{b'} \times r_4^b \end{bmatrix} \quad \text{each vector represents a row} \qquad 2.6.10$$

As before the optimal linear estimator of $\underline{\mu}$ is

$$\hat{\underline{\mu}} = (\beta^T\beta)^{-1} \beta^T \Delta\tau = \beta^+ \Delta\tau \qquad 2.6.11$$

and the estimated $\hat{\underline{\mu}}$ is used to update $C_i^{b'}$.

The actual calculation of this would be done most efficiently by Gaussian elimination; that is solving

$$(\beta^T\beta)\ \hat{\underline{\mu}} = \beta^T\ \Delta\tau \qquad 2.6.12$$

This and the basic algorithm can be approximately expressed in terms of each other. Linearizing the definition of τ about τ'

$$\tau = \cos\frac{V}{R}\,t \simeq \cos\frac{V}{R}\,t' - \frac{V}{R}(\sin\frac{V}{R}t')(t-t') \qquad 2.6.13$$

$$= \tau' - \frac{V}{R}\ (\sin\frac{V}{R}\,t')\ \Delta t \qquad 2.6.14$$

or

$$\Delta\tau = -\frac{V}{R}\ (\sin\frac{V}{R}\,t')\ \Delta t \qquad 2.6.15$$

This is fit into the vector form by defining a diagonal W matrix

$$W \triangleq \begin{bmatrix} -\frac{V}{R}\sin\left(\frac{V}{R}\,t'_{11}\right) & & & \\ & \ddots & & \\ & & \ddots & 0 \\ 0 & & & \ddots \\ & & & -\frac{V}{R}\sin\left(\frac{V}{R}\,t'_{24}\right) \end{bmatrix}$$

Thus

$$\underline{\Delta\tau} \approx W \, \underline{\Delta t} \qquad 2.6.17$$

Since

$$\sin \frac{V}{R} t'_{ij} = \left| d_i^{b'} \times r_j^{b} \right| \qquad 2.6.18$$

the matrix β of the basic algorithm may be factored

$$B = W^{-1}\beta \qquad 2.6.19$$

or equivalently

$$\beta = WB \qquad 2.6.20$$

Applying equations 2.6.17 and 2.6.20 to equation 2.6.8

$$W\underline{\Delta t} = WB\underline{\mu} \qquad 2.6.21$$

A solution of equation 2.6.21 by a pseudoinverse will minimize

$$\left| W(t - \hat{t}) \right| . \qquad 2.6.22$$

Thus the effect of this formulation is to weight the least squares procedure. The weighting varies with platform attitude. From equation 2.6.14 it weights the larger time measurements more heavily. Since the noise model has identical statistics for all the measurements the optimal weighting is uniform, i.e. W = I. Thus this weighted estimator is suboptimal with respect to mean square error.

This loss in performance is to be traded for a decrease in algorithm complexity. The algorithm that computes the weighted estimate is shown in the block diagram of Figure 2.3. The computation requirements are shown in Table 2.3. This is a reduction of 32 multiplies, 25 adds, 8 divisions and 8 square roots.

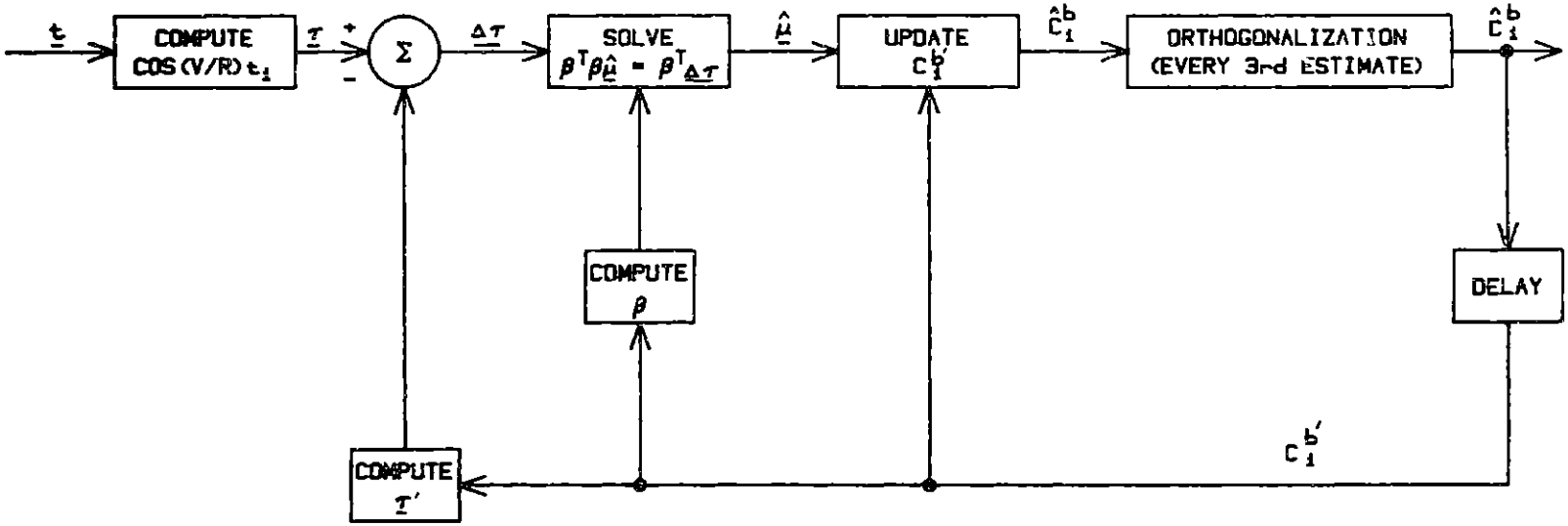

FIGURE 2.3 THE WEIGHTED ATTITUDE ESTIMATION ALGORITHM

Table 2.3

Computation Requirements

For the Weighted Algorithm

EQUATION	TIMES CALCULATED	MULTIPLIES	DIVISIONS	ADDS/SUBTRACTS	MISCEL-LANEOUS
2.6.2	8	8			8 cosines
2.1.3	2	18		12	
2.6.5	8	24		16	
2.6.10	1	48		24	
$\tau - \tau'$	1			8	
$\beta^T\beta$	1	72		63	
$\beta^T\Delta\tau$	1	24		21	
Gaussian elimination	1	11	6	11	
2.2.2	1	18		18	
Gram-Schmidt orthogonalization	*	9	1	7	1 square root
TOTAL		232	7	180	1 square root, 8 cosines

*Averaged over 3 iterations

III Algorithm Performance

The estimation algorithm's performance is degraded by three major error sources: noise, linearization, and use of an approximate update. A general evaluation of the error is based on independent analyses of each source. Analysis of error due to an approximate update was provided in section 2.4. Algorithm sensitivity and linearization error are analyzed in sections 3.1 and 3.2 respectively. The algorithm is simulated and the results are compared to the combination of the individual error analyses in section 3.3.

3.1 Noise Sensitivity Analysis

The noise sensitivity of the estimation algorithm characterizes the response of the algorithm to a noise input. Here, it is specifically the ratio of the rms value of the error of the output estimate to the rms value of the input noise.

The noise sources that corrupt the time measurements $\underline{t}$ are modeled as additive, zero mean and independent having equal variances due to the system symmetry. The noises are represented by the eight element vector $\underline{n}$ having a covariance matrix R.

$$R \triangleq E\left[\underline{n}\,\underline{n}^T\right] = \sigma_n^2 I \qquad 3.1.1$$

where σ_n is the rms value of the input noise.

The estimate of the incremental attitude $\underline{\mu}$ is computed by the pseudoinverse B^+ of equation 2.3.1. The response of the algorithm to noise is

$$\underline{\mu}_n = B^+ \underline{n}. \qquad 3.1.2$$

The characterization E of the error rotation $\underline{\mu}_n$ will be the rms value of its magnitude.

$$\varepsilon = |\mu_n| \qquad 3.1.3$$

The mean square value of the error is

$$E\left[\varepsilon^2\right] = E\left[\mathrm{tr}\left(\underline{\mu}_n \underline{\mu}_n^T\right)\right] \qquad 3.1.4$$

where tr( ) denotes the trace of a matrix.

$$E\left[\varepsilon^2\right] = E\left[\mathrm{tr}\left(B^+ \underline{n}\,\underline{n}^T B^{+T}\right)\right] \qquad 3.1.5$$

$$= \mathrm{tr}\left[B^+ E\left(\underline{n}\,\underline{n}^T\right) B^{+T}\right] \qquad 3.1.6$$

$$= \sigma_n^2 \,\mathrm{tr}\left(B^+ B^{+T}\right) \qquad 3.1.7$$

The rms value of the error is

$$\varepsilon_{rms} = \sigma_n \left(tr\left(B^+ B^{+T} \right) \right)^{1/2} \qquad 3.1.8$$

Thus the noise sensitivity S is

$$S = \left(tr\left(B^+ B^{+T} \right) \right)^{1/2} \qquad 3.1.9$$

For the basic algorithm

$$B^+ = \left(B^T B \right)^{-1} B^T \qquad 3.1.10$$

$$B^+ B^{+T} = \left(B^T B \right)^{-1} B^T B \left(B^T B \right)^{-1} \qquad 3.1.11$$

$$= \left(B^T B \right)^{-1} \qquad 3.1.12$$

Thus, for the basic algorithm

$$S = \left(tr\left(B^T B \right)^{-1} \right)^{1/2} \qquad 3.1.13$$

For the weighted algorithm from equations 2.6.11 and 2.6.17

$$\underline{\mu}_n = \beta^+ W \underline{n} \qquad 3.1.14$$

From the results above:

$$S = \left(tr\left(\beta^{+} W W^{T} \beta^{+T}\right)\right)^{1/2} \qquad 3.1.15$$

From equations 2.6.11 and 2.6.18:

$$S = \left(tr\left[\left(B^{T}W^{T}WB\right)^{-1} B^{T}W^{T}WW^{T}WB\left(B^{T}W^{T}WB\right)^{-1}\right]\right)^{1/2} \qquad 3.1.16$$

A lower bound on the optimum sensitivity may be obtained from a geometric argument. A measurement, t, between a driver $\underline{d}$ and a receiver $\underline{r}$ is a constraint on rotation about an axis defined by $\underline{d}x\underline{r}$. An error in t tends to perturb the vector representing the attitude estimate in the direction of $\underline{d}x\underline{r}$. It can be shown that a set of eight constraint directions, $\underline{d}_i x \underline{r}_j$, that produce the minimum magnitude of the error perturbation ε due to noises in all constraints, is represented by the corners of a cube centered at the origin.

The $\underline{d}_i x \underline{r}_i$ are also the directions of the rows of B, the linearized model. From equation 2.2.29, all rows of B have magnitude $\frac{R}{V}$; thus an optimal B based on the optimal set of directions above is

$$B_{LB} = \frac{1}{\sqrt{3}} \frac{V}{R} \begin{bmatrix} 1 & 1 & 1 \\ 1 & 1 & -1 \\ 1 & -1 & 1 \\ 1 & -1 & -1 \\ -1 & 1 & 1 \\ -1 & 1 & -1 \\ -1 & -1 & 1 \\ -1 & -1 & -1 \end{bmatrix} \qquad 3.1.17$$

Then

$$\left(B_{LB}^{T}B_{LB}\right)^{-1} = 3/8 \begin{bmatrix} 1 & 0 & 0 \\ 0 & 1 & 0 \\ 0 & 0 & 1 \end{bmatrix} \qquad 3.1.18$$

and the lower bound S_{LB} on the noise sensitivity is

$$S_{LB} = \sqrt{\frac{9}{8}}\,\frac{V}{R} \qquad 3.1.19$$

Using the specified values of V and R, S_{LB} is 4.20 x 10^{4} radians/sec. As the weighted algorithm is less optimal than the basic algorithm, this is also a lower bound for the weighted algorithm.

The sensitivities of both the basic and weighted algorithms were computed by equations 3.1.13 and 3.1.16 and plotted as a function of platform attitude as described by Euler angles. Only Euler angles between 0 and $\pi/4$ are considered. This eliminated redundancy since for an inertial frame as defined in Figure 1.2 the configuration of the drivers is symmetric about each axis by $\pi/4$. The sensitivity is displayed as a family of curves. The curves are indexed by the first rotation ϕ about the x axis and by the second rotation θ about the y axis. Each curve is a function of the third rotation ψ about the z axis. A pair of driver locations is chosen for the estimation, which have the greatest z component in the b frame. Changing pairs causes a discontinuity in the sensitivity.

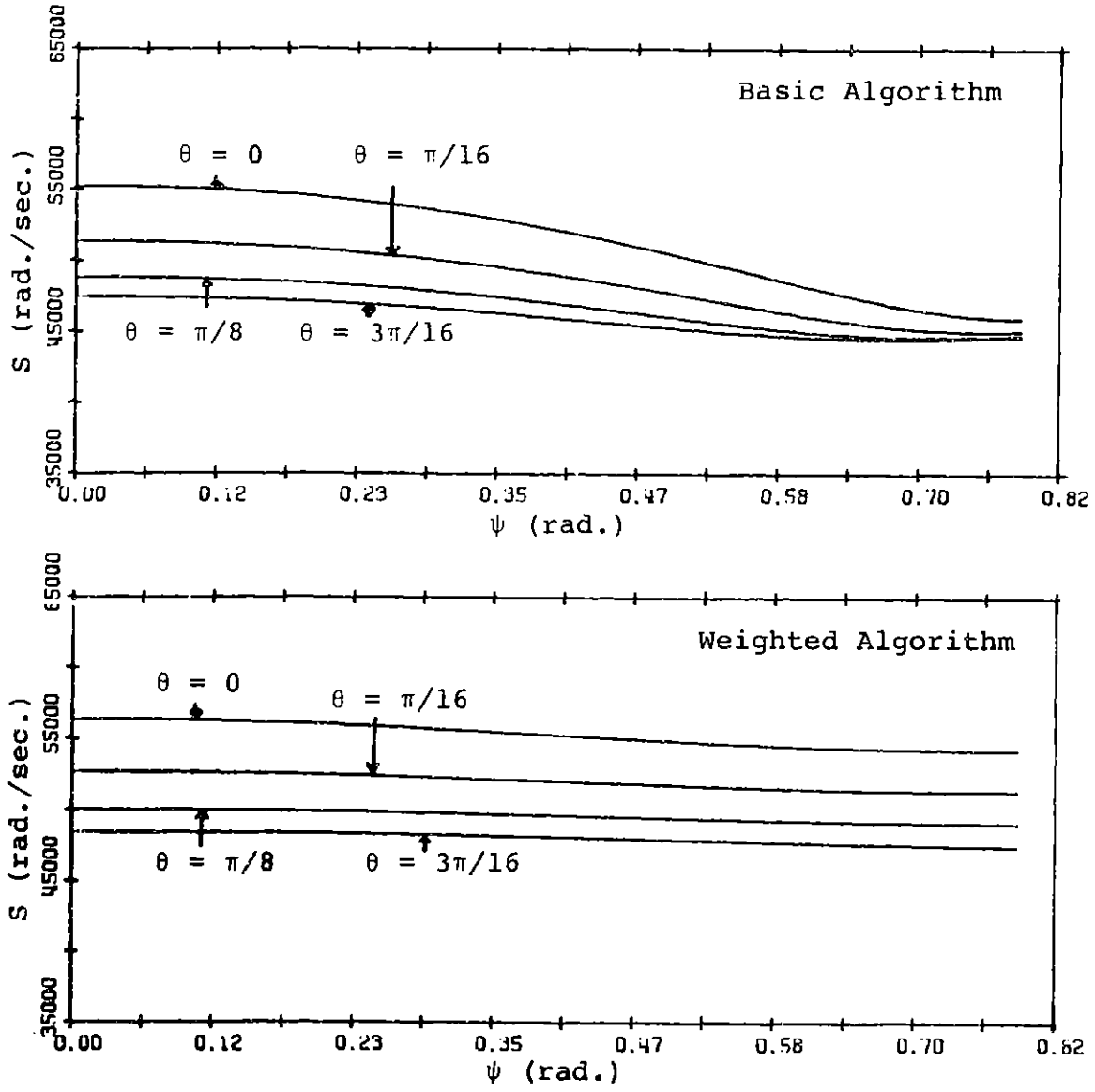

Figure 3.1 Sensitivity to Noise
(ϕ = 0)

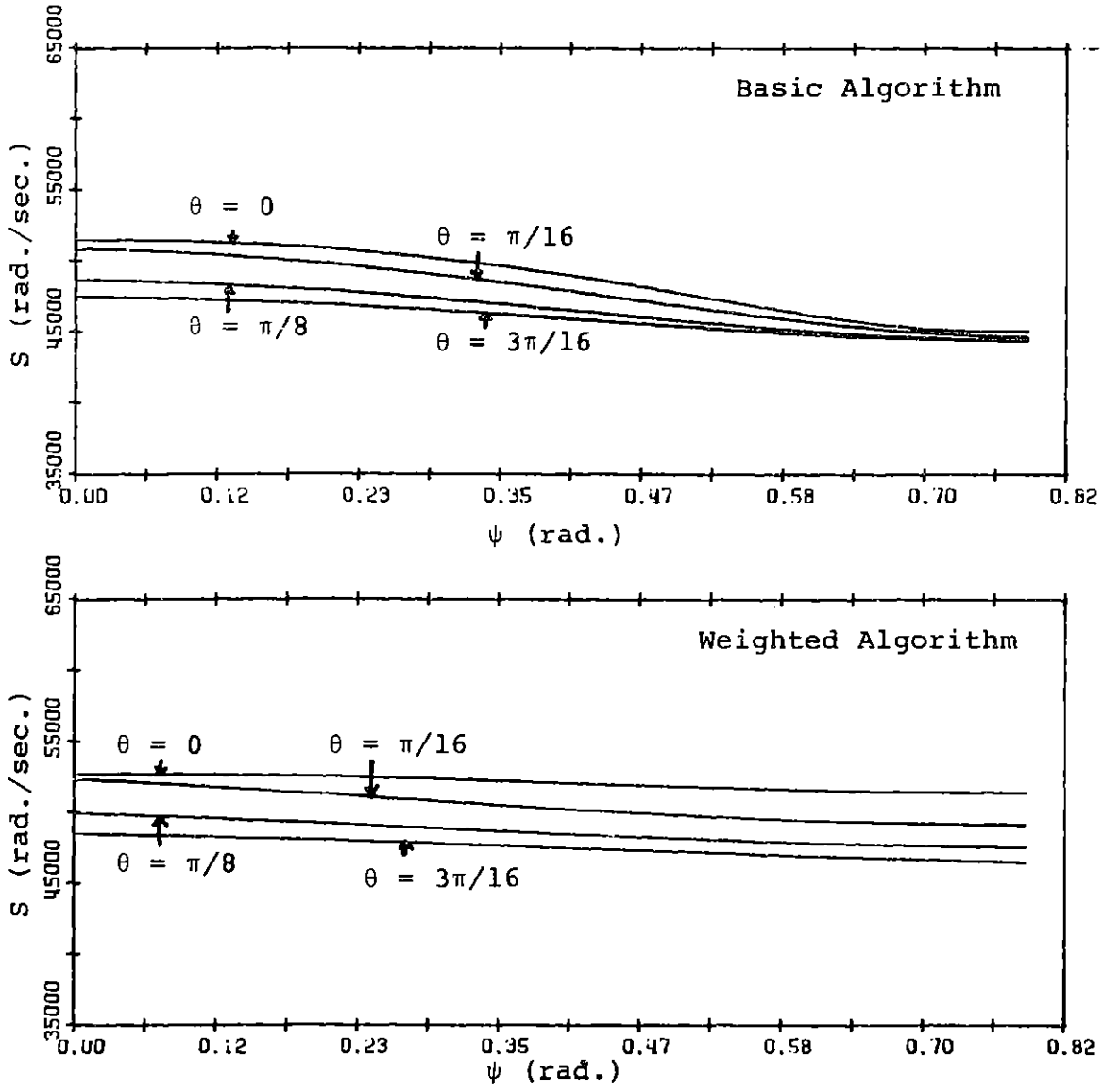

Figure 3.2 Sensitivity to Noise
($\phi = \pi/16$)

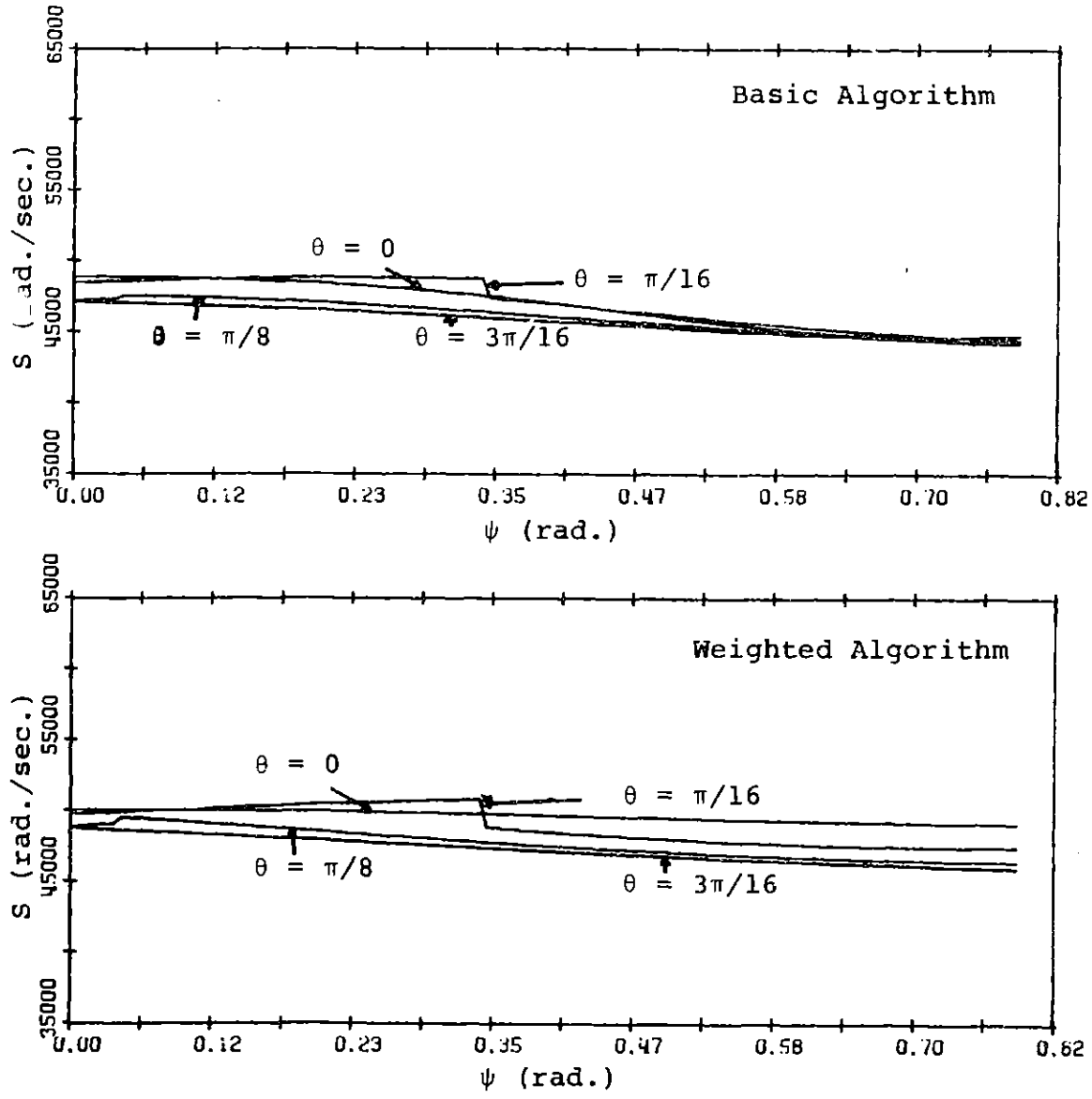

Figure 3.3 Sensitivity to Noise
($\phi = \pi/8$)

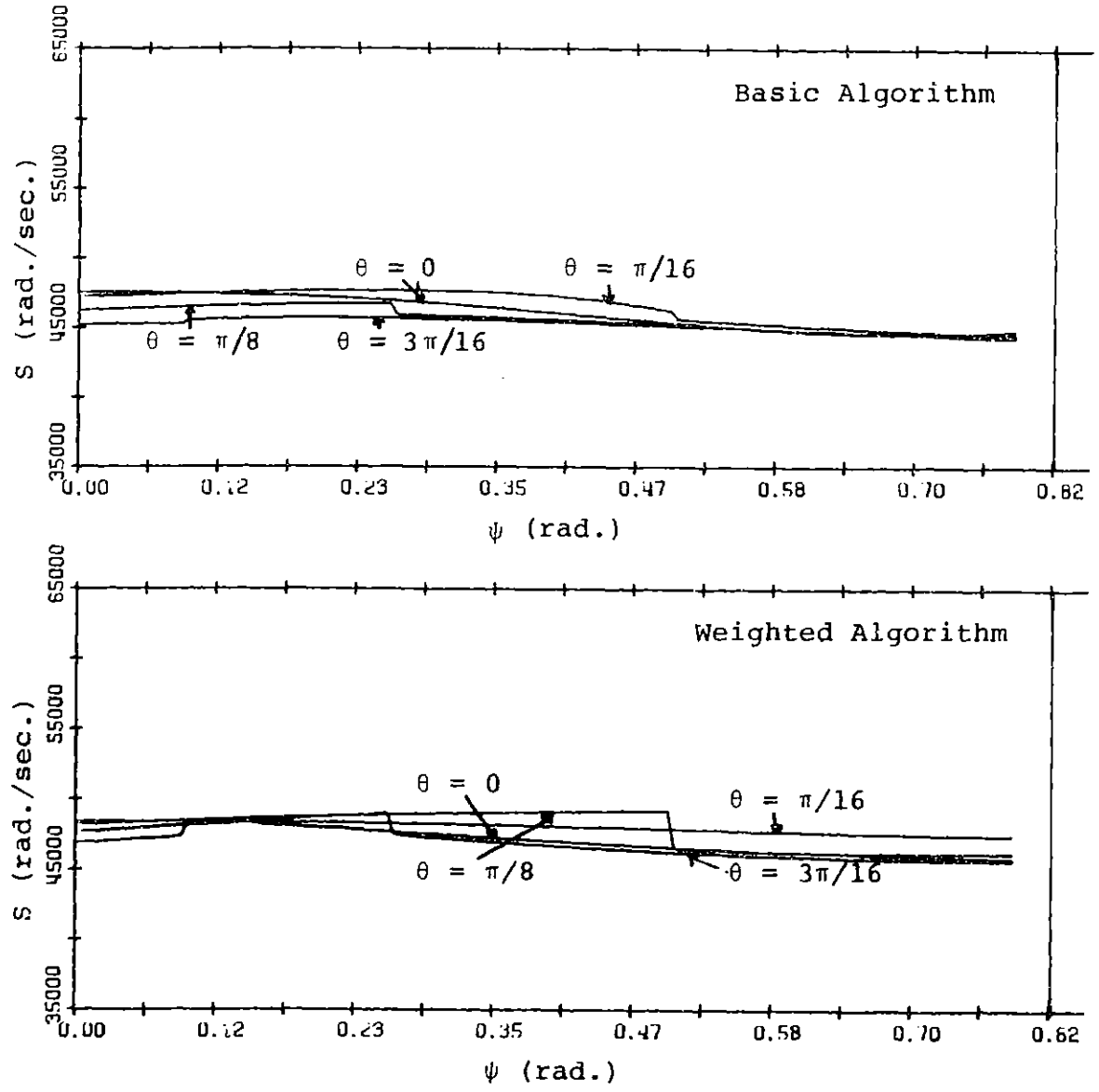

Figure 3.4 Sensitivity to Noise
($\phi = 3\pi/16$)

The RMS value of all the computed sensitivities was 4.88×10^4 which is 15 percent above the optimal value. However, the optimal value is valid for only a few attitudes; an RMS value considering all attitudes would be greater. The maximum and minimum values were 5.63×10^4 and 4.55×10^4 respectively; a range of 20 percent.

As expected, the sensitivity of the weighted algorithm is consistently greater than that of the basic algorithm. However, it represents an increase of typically seven percent and raises the maximum value by two percent. This minor increase will be traded for a savings in computation, and the remainder of the analysis in this chapter will deal only with the weighted algorithm.

3.2 Linearization Error

Linearization error is that error in the estimate arising from the use of a linear approximation in the algorithm development. Because of this approximation, the estimate will be in error even though the input time measurements may contain no noise.

Specifically, the linearization error ε_L is the magnitude of the rotation between $\underline{\mu}$ and $\hat{\underline{\mu}}$, where $\underline{\mu}$ and $\hat{\underline{\mu}}$ define C_b^b, and $\hat{C}_b^b$, by the series of equation 2.2.3 . The linearization error in the weighted

algorithm is the approximation of C_b^b, by I+M which is a truncation of $\sum_{k=0}^{\infty} \frac{M^k}{K!}$. The i^{th} element of this series has a norm of $(\sqrt{2}\,|\underline{\mu}|)^i/i!$, where the norm is defined as $(\mathrm{tr}M^TM)^{1/2}$. For small $|\underline{\mu}|$, the dominant truncated term is the second order term having a magnitude of $(\sqrt{2}/2)|\underline{\mu}|^2$. Thus ε_L will depend quadratically on $|\underline{\mu}|$, i.e.

$$\varepsilon_L = K|\underline{\mu}|^2 \qquad 3.2.1$$

where K is some constant. A closed form determination of K is infeasible as it requires a closed form solution of the original nonlinear problem. Thus, ε_L will be characterized computationally.

The linearization error for a true attitude C_i^b, which is composed of $C_i^{b'}$ and $\underline{\mu}$, is calculated by implementing the estimation of $\hat{\underline{\mu}}$ as shown in Figure 1. The model of equation 2.6. is used to calculate the propagation times $\underline{\tau}$ and $\underline{\tau}'$ for C_i^b and $C_i^{b'}$ respectively. The pseudoinverse B^+ is calculated for $C_i^{b'}$ from equations 2.6.10 and 2.6.11. Then $\hat{\underline{\mu}}$ is found by

$$\hat{\underline{\mu}} = B^+(\tau - \tau') \qquad 3.2.2$$

The rotation between $\underline{\mu}$ and $\hat{\underline{\mu}}$ is given by (see Appendix D)

$$\varepsilon_L = 2 \sin^{-1} \left| \cos \frac{\alpha}{2} \sin \frac{\hat{\alpha}}{2} \hat{\underline{\nu}} + \cos \frac{\hat{\alpha}}{2} \sin \frac{\alpha}{2} \underline{\nu} + \sin \frac{\alpha}{2} \sin \frac{\hat{\alpha}}{2} \hat{\underline{\nu}} X \underline{\nu} \right| \qquad 3.2.3$$

where

$$\alpha = |\underline{\mu}| \ , \quad \hat{\alpha} = |\hat{\underline{\mu}}| \qquad 3.2.4$$

$$\underline{\nu} = \frac{1}{\alpha} \underline{\mu}, \ \hat{\underline{\nu}} = \frac{1}{\hat{\alpha}} \hat{\underline{\mu}} \qquad 3.2.5$$

ε_L was computed for the nominal attitudes defined by the Euler angle sets (0,0,0) and ($\pi/8$,0,$\pi/4$). At each attitude, ε_L was computed for three directions $\underline{\nu}_1, \underline{\nu}_2$ and $\underline{\nu}_3$ of $\underline{\mu}$.

$$\underline{\nu}_1 = \begin{bmatrix} 1 \\ 0 \\ 0 \end{bmatrix} \quad \underline{\nu}_2 = \frac{1}{\sqrt{2}} \begin{bmatrix} 1 \\ 1 \\ 0 \end{bmatrix} \quad \underline{\nu}_3 = \frac{1}{\sqrt{3}} \begin{bmatrix} 1 \\ 1 \\ 1 \end{bmatrix} \qquad 3.2.6$$

Log (ε_L) is plotted against log (α) in figures 3.5 and 3.6. These curves are nearly straight with a slope of 2:1, which confirms the quadratic dependance of ε_L on α. The curves show little sensitivity of ε_L to direction $\underline{\nu}$ or nominal attitude. Thus the maximum observed

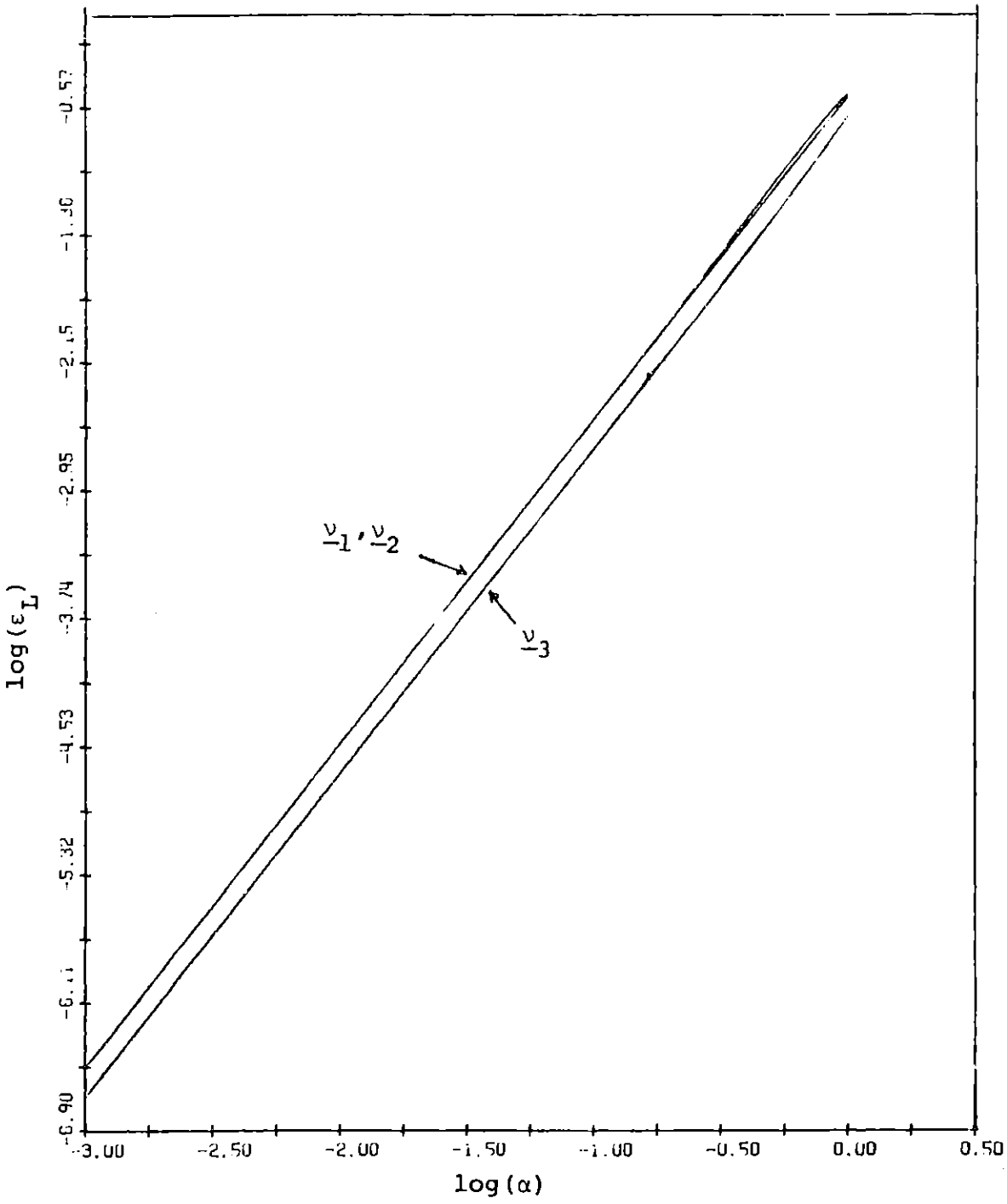

Figure 3.5 Linearization Error at (0,0,0)

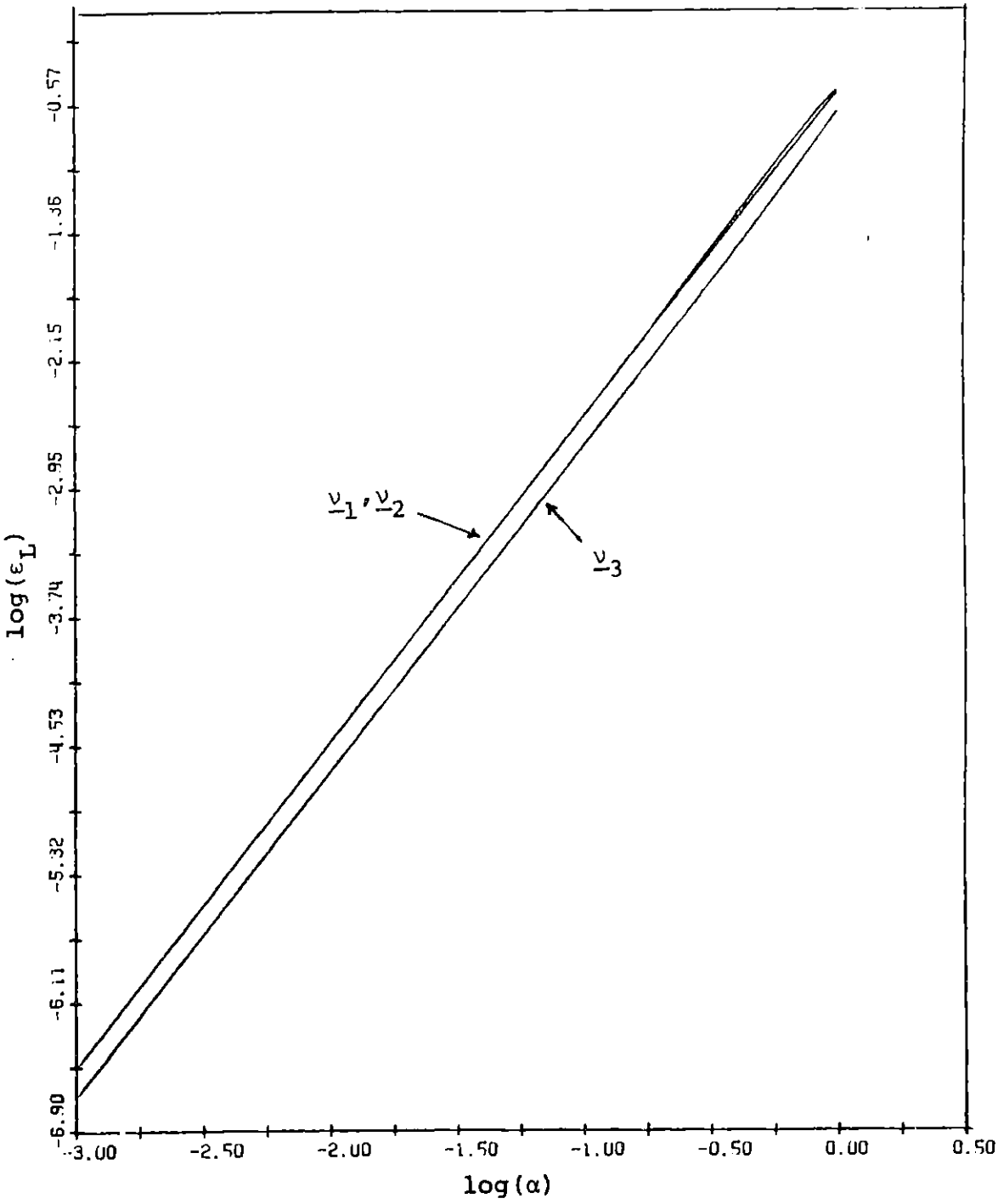

Figure 3.6 Linearization Error at $(\pi/4, \pi/4, \pi/4)$

value of K = .38 is likely to be close to its actual maximum value. Thus, for evaluation, it is reasonable to model ε_L as

$$\varepsilon_L = .38\alpha^2 \quad \alpha < 1 \text{ radian} \qquad 3.2.7$$

For the largest platform rotation between measurements, 20 mrad. the linearization error is .15 mrad. This is about 5% of the maximum allowable error.

These results indicate that even for relatively large angles, up to one radian, the linearization error is smaller than the inital error. This implies that if the algorithm were to be iterated while keeping the same input measurement, it will converge to an accurate estimate if the initial error α is less than a radian in magnitude.

3.3 Simulation

A simulation is useful for indicating the oversight of any significant error sources and checking the accuracy of the previous analysis. It also generates representative results.

The simulation implements the weighted algorithm according to Figure 2.3 . The simulated input to the algorithm is based on a sequence of true attitudes C_i^b. These C_i^b are generated by

$$C_i^b(K) = D(K)C_i^b(K-1) \qquad 3.3.1$$

where K is the index of the sequence. The matrix D is a rotation of magnitude equal to the maximum rotation of the platform between measurements, which is 20 milliradians. The axis of rotation of D is selected randomly. The propagation times, $\underline{t}$, are generated from the model of equation 2.4. and added with a noise vector $\underline{n}$. $\underline{n}$ has the properties assumed in section 2.3; it is normally distributed with zero mean and covariance matrix σ_n^2, where σ_n is the specified maximum rms value of the input noise, 1×10^{-8} seconds.

As the simulation will use a first order update matrix, the estimate $\hat{C}_i^b$ will not generally be orthogonal. Thus, the error will be analyzed as defined in Appendix C. The error is the maximum singular value of $C_i^b - \hat{C}_i^b$.

The results of the simulation for a few arbitrarily chosen initial attitudes $C_i^b(0)$ are shown in the plots of Figure 3.7. . The rms values of the error for each of these simulations is shown in Table 3.1.

For comparison, the errors due to each of the three major sources were also computed. The rms error due to noise is given by the input rms noise level, 1×10^{-8} seconds, multiplied by the algorithm's sensitivity as computed by equation 3.1.15. The linear-

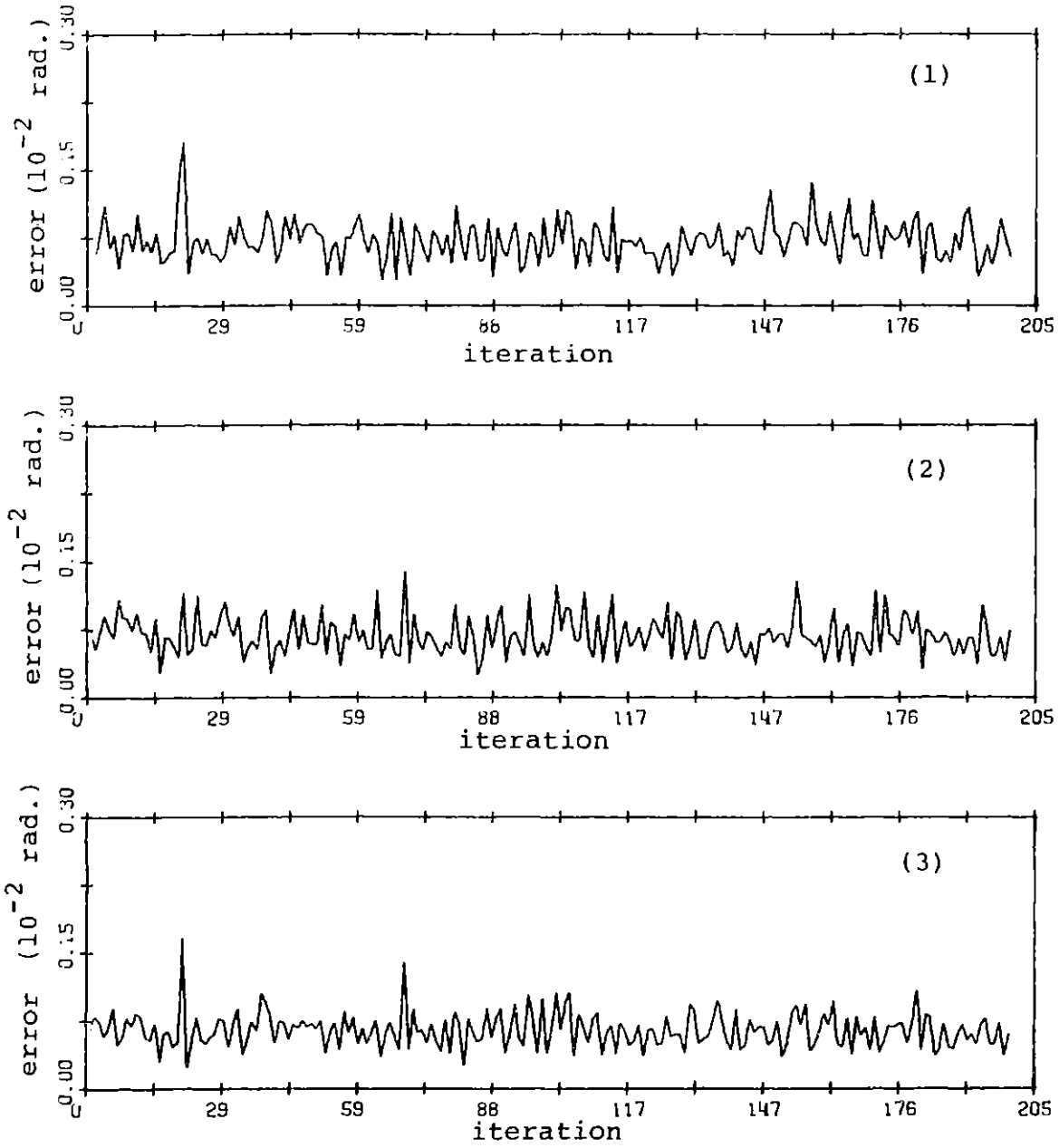

Figure 3.7 Algorithm Simulations

ization error is computed from equation 3.2.7 for a 20 milliradian platform rotation between measurements. $\hat{C}_i^b$ is re-orthogonalized every third iteration. As shown in section 2.4, an upper bound on the update error is $\cdot 20$ milliradians for the first iteration after orthogonalization, and then .40 and .60 milliradians on the next two iterations. The rms value of this sequence of upper bounds is .432 milliradians.

The combination of these individual results depends upon their statistical relationships. If the error sources are uncorrelated, then the errors are combined in a rms sense. A worst case combination assumes that all errors are in the same direction and the composite magnitude is the algebraic sum of the individual magnitudes. Both combinations are included in Table 3.1.

The results of each simulation fall between the two computed composite errors, but much closer to the composite error based on the assumption that its components are uncorrelated. That the computed and simulated errors have the same relative sizes further substantiates the validity of the analysis. Also, assuming a worst case error of three times the rms error, the simulation results indicate that the weighted algorithm will surpass its specified performance.

Table 3.1 Simulation Error Analysis*

Simulation	Initial Attitude (Euler angles)	RMS Noise Error	RMS Linearized Error	RMS Update Error	Uncorrelated Composite Error	"Worst Case" Composite Error	RMS Simulated Error
1	(0,0,0)	.576	.153	.436	.736	1.008	.773
2	(π/8,0,π/4)	.491	.155	.432	.671	.923	.704
3	(π/4,π/4,π/4)	.472	.153	.432	.658	.904	.681

*All errors are expressed in milliradians

IV Implementation Considerations

This chapter addresses some of the major considerations for the implementation of the algorithm developed in chapter 2.

The first section develops an initialization procedure. As the algorithm is developed from a linearized model, it requires a nominal attitude upon which to base its linearization. This nominal attitude is normally taken to be the previous attitude estimate; however when the algorithm is started it has no previous estimate. Thus, as initialization procedure is required to determine platform attitude to an accuracy that will not cause excessive linearization error in the main algorithm.

It is anticipated that there might be error in some parameters of the model that cannot be removed by calibration. To avoid error due to an inaccurate model the uncertain parameters must be estimated along with the attitude. Section 4.3 presents the extensions of the basic algorithm developed in chapter 2 to include estimation of additional parameters, velocity and measurement time biases.

4.1 Initialization

This initialization procedure is based on the property of the DCM C_i^b that the columns of C_i^b are the base vectors of the i frame as represented in the b frame. The representation of a vector v in the b frame is the dot product of v with the base vectors of the b frame.

$$\underline{v}^b = \begin{bmatrix} \underline{I}^b \cdot \underline{v} \\ \underline{J}^b \cdot \underline{v} \\ \underline{K}^b \cdot \underline{v} \end{bmatrix} \qquad 4.1.1$$

If there were receivers r_a, r_b, and r_c whose position vectors coincided with the orthogonal basis of the frame $\underline{I}^b$, $\underline{J}^b$, $\underline{K}^b$ then the representation of a driver's position could be obtained from the measured times, t_{ij}

$$\underline{d}^b = \begin{bmatrix} \underline{r}_a \cdot \underline{d}_a \\ \underline{r}_b \cdot \underline{d}_a \\ \underline{r}_c \cdot \underline{d}_a \end{bmatrix} = \begin{bmatrix} \cos\frac{V}{R} t_{aa} \\ \cos\frac{V}{R} t_{ab} \\ \cos\frac{V}{R} t_{ac} \end{bmatrix} \qquad 4.1.2$$

However, such a configuration is not available as no receiver position vector is orthogonal to another; each pair of adjacent receivers forms an angle of 84°. Thus a new body-fixed frame $\tilde{b}$ is defined by application of the Gram Schmidt procedure to two receiver vectors $\underline{r}_i$ and $\underline{r}_j$ (see figure 4.1).

$$\underline{I}^{\tilde{b}} = \underline{r}_i \qquad 4.1.3$$

$$\underline{J}^{\tilde{b}} = (\underline{r}_j - p_r \, r_i)/q_r \qquad 4.1.4$$

$$p_r = \underline{r}_i \cdot \underline{r}_j \qquad 4.1.5$$

$$q_r = |\underline{r}_j - p_r \, \underline{r}_i| \qquad 4.1.6$$

$$\underline{K}^{\tilde{b}} = \underline{I}^{\tilde{b}} \times \underline{J}^{\tilde{b}} \qquad 4.1.7$$

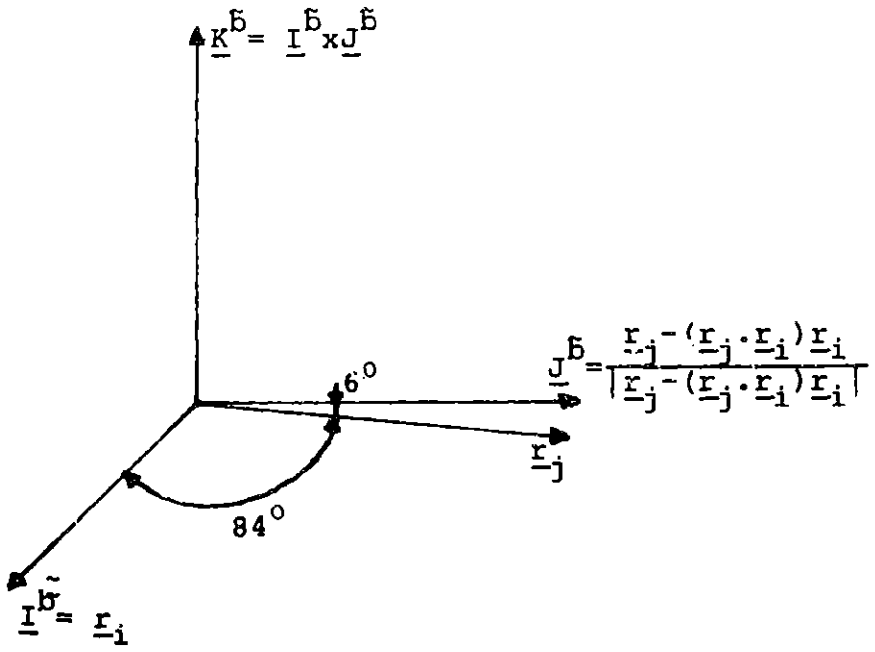

Figure 4.1 $\mathfrak{b}$ Frame Construction

The representation $\underline{d}_i^{\tilde{b}}$ of a driver i in the $\tilde{b}$ frame may now be calculated from the time measurements. The x component $d_x^{\tilde{b}}$ of $\underline{d}_i^{\tilde{b}}$ is given by

$$d_x^{\tilde{b}} = \underline{I}^{\tilde{b}} \cdot \underline{d}_i = \underline{r}_i \cdot \underline{d}_i = \cos \frac{V}{R} t_i \qquad 4.1.8$$

where t_i is the time measurement between $\underline{d}$ and $\underline{r}_i$.

The y component is found from Eq. 4.1.4 by

$$d_y^{\tilde{b}} = \underline{J}^{\tilde{b}} \cdot \underline{d}^{\tilde{b}} = \left[(\underline{r}_j - p_r \underline{r}_i)/q_r\right] \cdot \underline{d} \qquad 4.1.9$$

$$= (\underline{r}_j \cdot \underline{d} - p_r \underline{r}_i \cdot \underline{d})/q_r \qquad 4.1.10$$

$$= (\cos \frac{V}{R} t_j - p_r \cos \frac{V}{R} t_i)/q_r \qquad 4.1.11$$

The magnitude of $d_z^{\tilde{b}}$ is obtained from the fact that $\underline{d}^{\tilde{b}}$ must be a unit vector. The sign of $d_z^{\tilde{b}}$ is determined from the implicit knowledge that a driver lies in the hemisphere of the receivers above the damping band; otherwise it would produce no measurement. If the r_i and r_j are chosen to be adjacent and ordered so that $\underline{r}_i \times \underline{r}_j$, which is the direction of $K^{\tilde{b}}$, is also in the receivers' hemisphere then the hemisphere of positive z component in the $\tilde{b}$ frame includes nearly all of the region in which a driver may produce a detectable pulse. The exceptions are avoided by careful selection of receivers i and j. Thus the sign of $d_z^{\tilde{b}}$ is positive and

$$d_z^{\tilde{b}} = \sqrt{1 - (d_x^{\tilde{b}})^2 + (d_y^{\tilde{b}})^2} \qquad 4.1.12$$

If there were three drivers d_1, d_2, and d_3 that coincided with the base vectors of the i frame, computation of $C_{\tilde{i}}^{\tilde{b}}$ would be the calculation of

$$C_{\tilde{i}}^{\tilde{b}} = \left[\underline{d}_1^{\tilde{b}} \cdot \underline{d}_2^{\tilde{b}} \cdot \underline{d}_3^{\tilde{b}}\right] \qquad 4.1.13$$

where the $\underline{d}_i^{\tilde{b}}$ are calculated by the equations 4.8, 4.11, and 4.12. Due to the presence of the damping band, such a configuration isn't available without increasing the number of drivers.

Thus a new inertial frame $\tilde{i}$ is defined by the application of the Gram Schmidt procedure to two driver vectors. This definition is similar to that of the $\tilde{b}$ frame (see figure 4.1).

$$\underline{I}^{\tilde{i}} = \underline{d}_i \qquad 4.1.14$$

$$\underline{J}^{\tilde{i}} = (\underline{d}_j - p_d\, \underline{d}_i)/q_d \qquad 4.1.15$$

$$p_d = \underline{d}_i \cdot \underline{d}_j \qquad 4.1.16$$

$$q_d = |\underline{d}_j - p_d\, \underline{d}_i| \qquad 4.1.17$$

$$\underline{K}^{\tilde{i}} = \underline{I}^{\tilde{i}} \times \underline{J}^{\tilde{i}} \qquad 4.1.18$$

Note that when $\underline{d}_i$ and $\underline{d}_j$ are chosen to be adjacent p_d and q_d are constants.

Now the transformation $C_{\tilde{i}}^{\tilde{b}}$ between the i and b frames are calculated by

$$C_{\tilde{i}}^{\tilde{b}} = \left[\underline{d}_i^{\tilde{b}} \;\vdots\; (\underline{d}_j^{\tilde{b}} - p_d \underline{d}_i^{\tilde{b}})/q_d \;\vdots\; \underline{d}_i^{\tilde{b}} \times (\underline{d}_j^{\tilde{b}} - p_d \underline{d}_i^{\tilde{b}})/q_d \right] \qquad 4.1.19$$

The computation required to compute $C_{\tilde{i}}^{\tilde{b}}$ from the time measurements is only 24 multiples, 12 adds, 4 cosines, and 2 square roots.

To utilize $C_{\tilde{i}}^{\tilde{b}}$ it is necessary to have the transformation $C_{i}^{\tilde{i}}$ from the i frame to the $\tilde{i}$ frame and the transformation $C_{\tilde{b}}^{b}$ from the $\tilde{b}$ frame to the b frame so that C_i^b may be computed as

$$C_i^b = C_{\tilde{b}}^{b} \; C_{\tilde{i}}^{\tilde{b}} \; C_{i}^{\tilde{i}} \qquad 4.1.20$$

The columns of $C_{\tilde{b}}^{b}$ are the axes of the $\tilde{b}$ frame as represented in the b frame. Thus

$$C_{\tilde{b}}^{b} = \left[\underline{r}_i^b \;\vdots\; (\underline{r}_j^b - p_r \underline{r}_i^b)/q_r \;\vdots\; \underline{r}_i^b \times (\underline{r}_j^b - p_r \underline{r}_i^b)/q_r \right] \qquad 4.1.21$$

$C_{i}^{\tilde{i}}$ is similarly computed as its rows are the axes of the $\tilde{i}$ frame as represented in the i frame. Thus

$$C_{i}^{\tilde{i}} = \begin{bmatrix} \underline{d}_i^{iT} \\ - - - - - - - - - - - \\ (\underline{d}_j^i - p_d \underline{d}_i^i)^T/q_d \\ - - - - - - - - - - - \\ (\underline{d}_i^i \times (\underline{d}_j^i - p_d \underline{d}_i^i)/q_d)^T \end{bmatrix}$$

With regard to computational load it should be noted that $C_{\tilde{b}}^{b}$ and $C_{i}^{\tilde{i}}$ need only be recomputed when new receivers or drivers are chosen.

The total computational requirement for this initialization procedure is 102 multiples, 60 adds, 4 cosines, and 2 square roots. In comparison this is about one third of the requirements for one iteration of the main algorithm.

As mentioned above, the receivers r_i and r_j must be selected so as to maintain the validity of the assumption that a driver used by this procedure has a positive $\tilde{z}$ component in the $\tilde{b}$ frame. Assuming that a pair of drivers are selected based on audibility (positioned to produce a detectable pulse) then any driver may be selected that lies in the receivers' hemisphere above the damping band. The area in this region that has a negative $\tilde{z}$ component is illustrated in figure 4.2.

This figure shows that in order for the driver to fall into that region, the receivers forming the $\tilde{b}$ frame must be the closest receivers to that driver. The approach to receiver selection is then to choose the receivers furthest away from the drivers. This criterion is readily available from the time measurements. First, a receiver is chosen for test from any driver by identifying the driver receiver pair d_1, r_1 associated with the largest time measurement. Then the receiver adjacent to r_1 having the greater distance to the other driver d_2 is

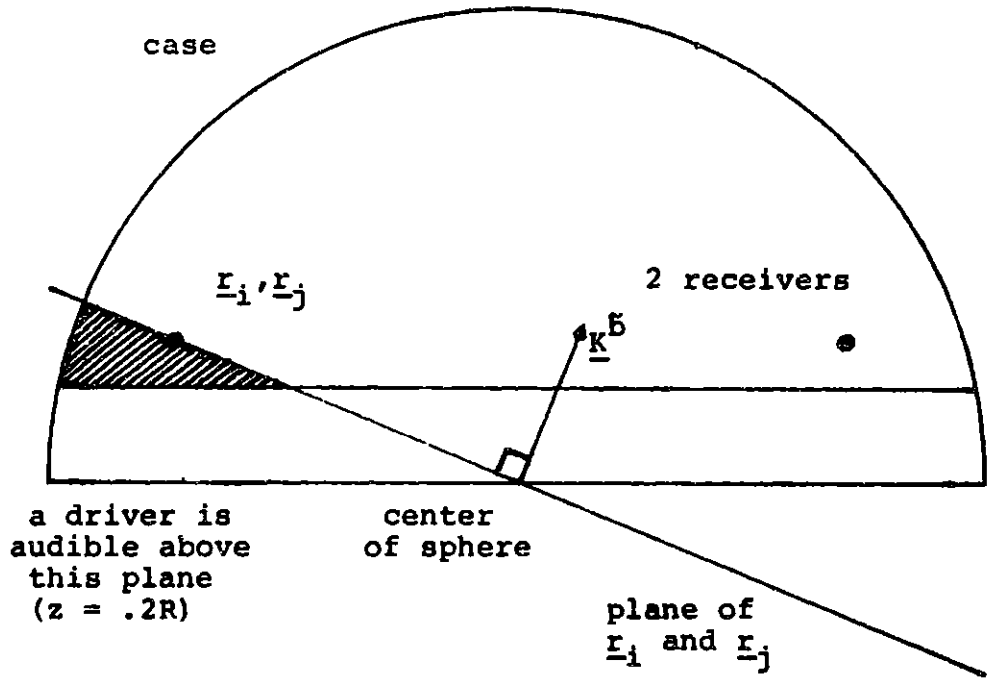

Figure 4.2 Positive $\tilde{z}$ Assumption Failure

chosen. The selection process is completed by ordering r_1 and r_2 so that the resulting $\underline{K}^b$ is in the receiver's hemisphere.

In order to verify the validity of the initialization procedure and test it for sensitivity to noise and computation error, it was simulated. The simulated platform attitudes were generated randomly for each trial by normalizing a vector of four numbers obtained from a zero mean gaussian random number generator, and interpreting them as a quaternion. Two drivers are then selected by their audibility, i.e., if the z component of a driver's position in the b frame was greater than 0.2 R it was assumed to be sufficiently clear of the damping band to excite a measureable pulse. This definition of audibility allows selection of drivers 0.1 R below the plane defined by the four receivers. Two receivers were selected as described above. Pulse propagation times were computed by the model of equation 2.1.4. The error was evaluated based on the maximum singular value of $C_i^b - \hat{C}_i^b$.

The results of a simulation with no noise are shown in figure 4.3a. These disclose no numerical sensitivities and verify the receiver selection criteria. Figure 4.3b shows the error resulting from the addition of noise with the specified rms level of 1×10^{-8} seconds to the simulated pulse propagation times. The rms value of the

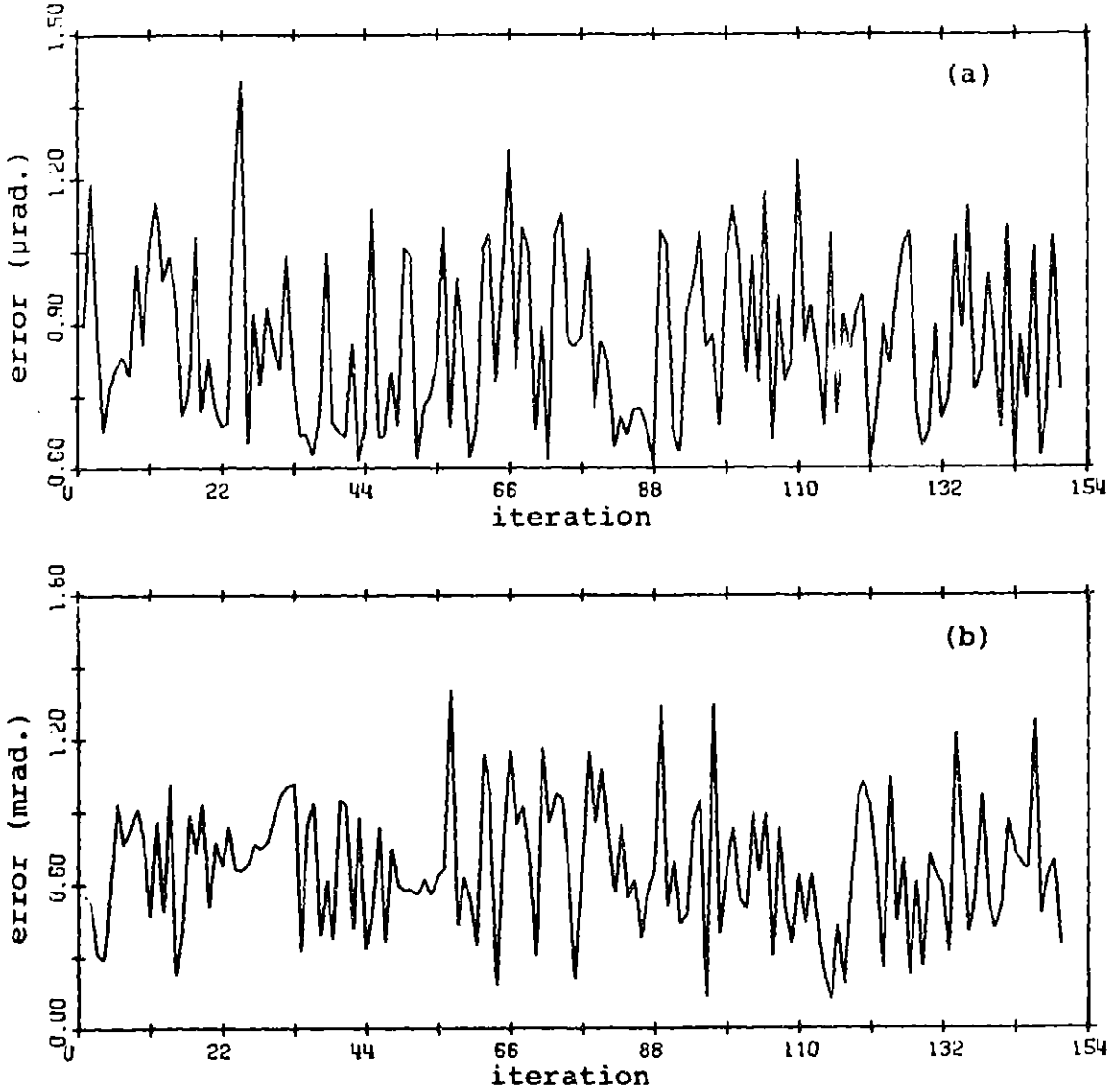

Figure 4.3 Initialization Procedure Simulations

resulting error was 0.704 milliradians. This performance is comparable with that of the main algorithm and will easily satisfy its initialization requirements. Because of its low computation requirement this algorithm should be considered for use as the main algorithm in future study.

4.2 Estimation of Additional Parameters

The following subsections present the inclusion of velocity and time measurement biases into the estimation.

4.2.1 Estimation of Velocity Bias

There can be error in the model's velocity parameter caused by variations in the acoustic velocity of the case due to temperature and stress. Inclusion of this parameter into the estimation still leaves the redundancy required for estimation. This development parallels much of the development of chapter 2.

From equation 2.1.4 the model is

$$t = \frac{R}{V} \cos^{-1}(\underline{r}^b \cdot C_i^b \, \underline{d}^i) \qquad 4.2.1$$

Using the approximation of equation 2.2.6

$$t = \frac{R}{V} \cos^{-1}(\underline{r}^b \cdot \underline{d}^{b'} + \underline{r}^b \cdot M\underline{d}^{b'}) \qquad 4.2.2$$

where $d^{b'} = C_i^{b'} d^i$. From equation 2.2.

$$t = \frac{R}{V} \cos^{-1}(\underline{r}^b \cdot \underline{d}^{b'} + (\underline{d}^{b'} \times \underline{r}^b) \cdot \underline{\mu}) \qquad 4.2.3$$

Linearizing about the nominal $V = V'$, $\underline{\mu} = 0$

$$t = \frac{R}{V'}\cos^{-1}(\underline{r}^b \cdot \underline{d}^{b'}) - \frac{R}{(V')^2}\cos^{-1}(\underline{r}^b \cdot \underline{d}^{b'})\Delta V$$

$$- \frac{R}{V'}\left(1 - (\underline{r}^b \cdot \underline{d}^{b'})^2\right)^{-1/2}(\underline{d}^{b'} \cdot \underline{r}^b) \cdot \underline{\mu} \qquad 4.2.4$$

where $\Delta V = V - V'$

Letting t' be the nominal time that would be obtained from the model if $C_i^b = C_i^{b'}$ and using equation 2.2.4

$$t = t' - \frac{t'}{V'}\Delta V - \frac{R}{V'}\frac{(\underline{d}^{b'} \times \underline{r}^b)}{|\underline{d}^{b'} \times \underline{r}^b|} \cdot \underline{\mu} \qquad 4.2.5$$

or

$$\Delta t = t - t' = -\frac{R}{V'}\frac{(\underline{d}^{b'} \times \underline{r}^b)}{|\underline{d}^{b'} \times \underline{r}^b|} \cdot \underline{\mu} - \frac{t'}{V'}\Delta V \qquad 4.2.6$$

Using the definitions of chapter 2

$$\Delta t_{ij} = -\frac{R}{V'}\frac{(\underline{d}_i^{b'} \times \underline{r}_j^b)}{|\underline{d}_i^{b'} \times \underline{r}_j^b|} \cdot \underline{\mu} - \frac{t'_{ij}}{V'}\Delta V \qquad 4.2.7$$

Combining all measurements into a compact matrix notation

$$\left[B \quad -\frac{1}{V'}\underline{t}'\right]\left[-\frac{\underline{\mu}}{\Delta V}\right] = \Delta t \qquad 4.2.8$$

where B is defined in equation 2.29, $\underline{\Delta t}$ is defined in equation 2.28 and

$$\underline{t'} = \begin{bmatrix} t_{11}' \\ t_{12}' \\ \vdots \\ t_{24}' \end{bmatrix} \qquad 4.2.9$$

$$\text{Let} \quad B_V = \left[B \quad -\frac{1}{V'} \underline{t}' \right] \qquad 4.2.10$$

$$\text{and} \quad \underline{\mu}_V = \begin{bmatrix} \underline{\mu} \\ \Delta V \end{bmatrix} \qquad 4.2.11$$

Then equation 4.2.8 becomes

$$B_V \underline{\mu}_V = \underline{\Delta t} \qquad 4.2.12$$

This is solved as before by a pseudo inverse

$$\hat{\underline{\mu}}_V = (B_V^T B_V)^{-1} B_V^T \underline{\Delta t} \qquad 4.2.13$$

Unlike the basic algorithm of chapter 2 the sub-optimal weighted version of the algorithm above offers no savings in computation. This is because while the weighting was implicit in the weighted algorithm here it must be explicitly applied to the column of B_V corresponding to the velocity bias.

The computational requirements of this algorithm are presented in Table 4.1.

Table 4.1 Computation Requirements for the Algorithm Extended for Velocity Bias.

equation	times calculated	multiplies	divisions	add/subtracts	miscellaneous
2.1.3	2	18		12	
4.2.1	8	32	8	16	8 $\cos^{-1}$
4.2.8	1	80	8	40	8 square roots
$\frac{t'}{V'}$	8	8	1		
$\underline{t} - \underline{t}'$	1			8	
$B_v{}^T B_v$	1	128		112	
$B_v{}^T \underline{\Delta t}$	1	32		28	
Gaussian elimination	1	26	10	26	
2.2.2	1	18		18	
Gram Schmidt orthogonalization*		9	1	7	1 square root
Total		351	28	267	9 square roots, 8 $\cos^{-1}$

*averaged over three iterations

The noise sensitivity of this extended algorithm was computed as a means of evaluation. The expression for the sensitivity is developed as in section 3.1. The covariance matrix P_v for $\hat{\underline{\mu}}_v$ is (see equation 3.1.11)

$$P_v = (B_v^T B_v)^{-1} \sigma_n^2 \qquad 4.2.14$$

The first three diagonal terms of P_v are the variances of the elements of $\underline{M}$ due to noise. The rms value of the magnitude α of $\underline{M}$ is

$$\alpha_{rms} = \sqrt{P_v(1,1) + P_v(2,2) + P_v(3,3)} \qquad 4.2.15$$

Thus the noise sensitivity of α, S_α is

$$S_\alpha = \alpha_{rms}/\sigma_n \qquad 4.2.16$$

The last diagonal term $P_v(4,4)$ is the mean square error in ΔV due to noise; and the noise sensitivity $S_{\Delta V}$ of $\hat{\Delta V}$ is

$$S_{\Delta V} = \sqrt{P_v(4,4)}/\sigma_n \qquad 4.2.17$$

The sensitivities of α and ΔV are computed by equations 4.2.16 and 4.2.17 and plotted as a function of platform attitude, as described by the Euler angle set (ϕ, θ, ψ), and nominal velocity. For a particular nominal velocity the sensitivity is plotted in two curves where each curve is a function of ψ. The two curves correspond to the pair of Euler angles ϕ, θ being 0, 0 and $\pi/4$, $\pi/4$.

These two pairs specify the curves in figures 3.1 and 3.4 that contain the maximum and minimum sensitivities of the basic algorithm. As this algorithm and the basic algorithm have the same system geometry, their maximum and minimum sensitivities should occur at the same respective attitudes. The sensitivity of α is shown for two nominal velocities, 198,000 inches per second, as specified, and 200,000 inches per second, which represents an anticipated 1 percent deviation in figures 4.4a and 4.4b respectively. Similarly, the sensitivity of ΔV is shown in figure 4.5.

The attitude sensitivity of this algorithm is about five percent higher than that of the basic algorithm. This loss in performance is to be compared with the error in the estimates from the basic algorithm due to a velocity bias. Preliminary results indicate that for an anticipated 2% error in the nominal velocity the extended algorithm is required to provide specified accuracy. A detailed analysis is left to further study.

4.2.2 Extension for a Driver Bias

Each driver can have a time measurement error bias, t^b. This error would be caused by variations in the gap between the driver and the case. Because this bias effects each measurement made with the same driver equally, redundant measurements can be used to accurately estimate the bias.

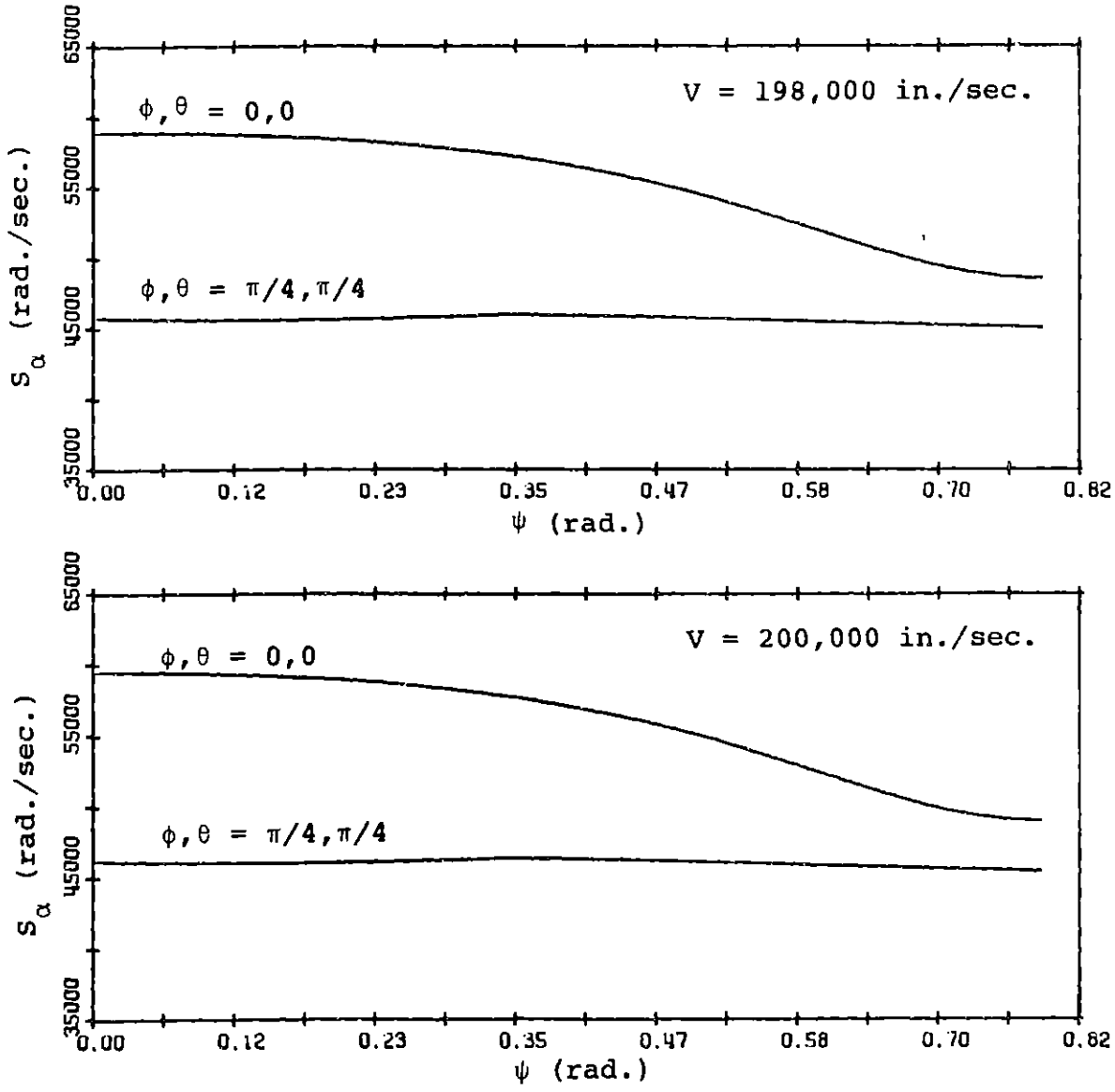

Figure 4.4 Noise Sensitivity of Attitude Estimates of the Algorithm Extended for Velocity Bias

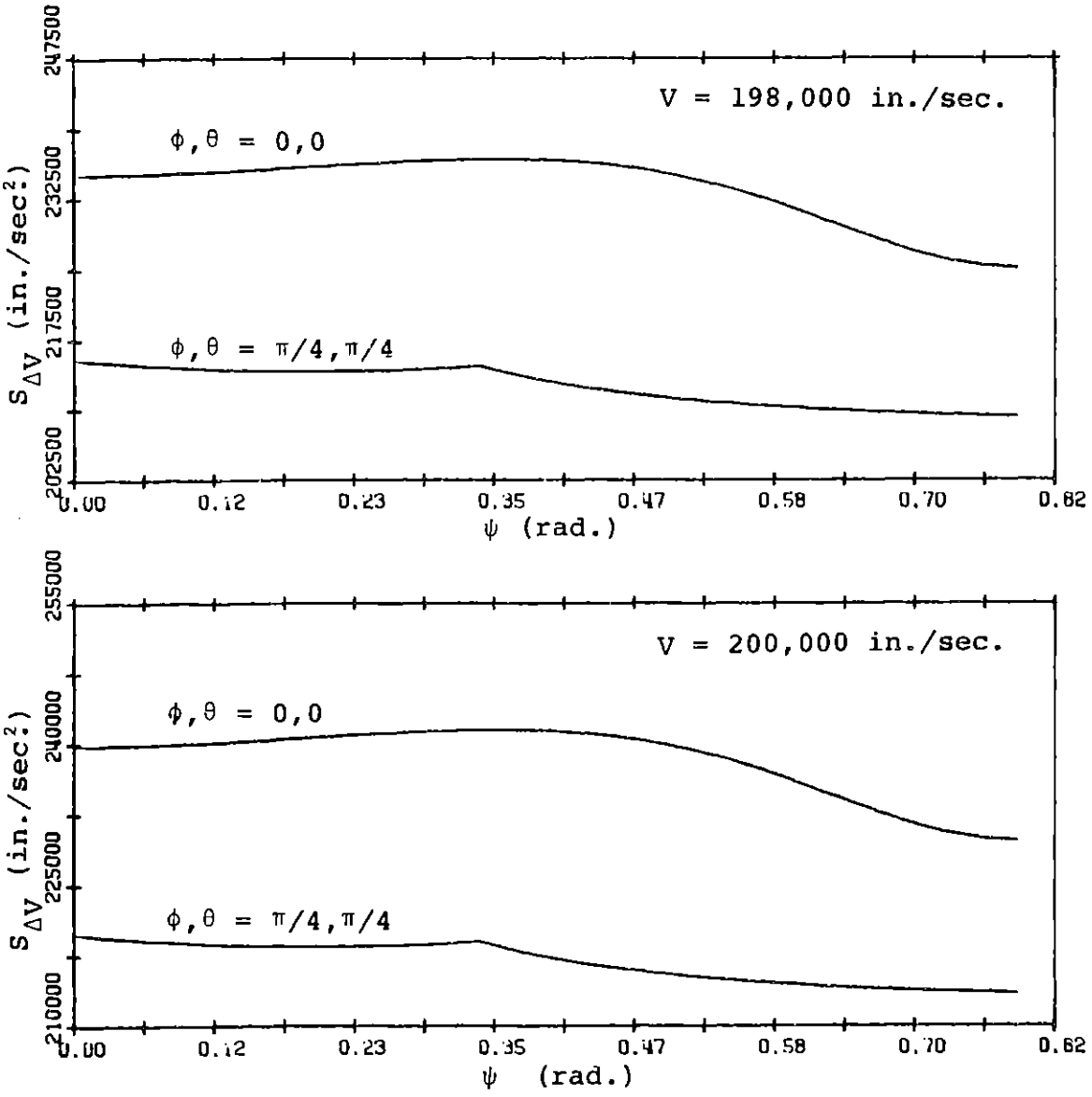

Figure 4.5 Noise Bias Sensitivity of Velocity Estimates

The bias for driver i is incorporated into the model of equation 2.4

$$t_{ij} = t_i^b + \frac{R}{V} \cos^{-1} (\underline{r}_j^b \cdot C_i^b \, \underline{d}_i^i) \qquad 4.2.18$$

This bias has no effect on the remainder of the linearized model. From equation 2.26

$$t_{ij} = t_i^b + t'_{ij} - \frac{R}{V} \frac{(\underline{d}_i^{b'} \times \underline{r}_j^b)}{|\underline{d}_b^{b'} \times \underline{r}_j^b|} \cdot \underline{\mu} \qquad 4.2.19$$

Combining all measurements into a compact matrix notation

$$B_T \underline{\mu}_T = \underline{\Delta t} \qquad 4.2.20$$

where

$$B_T \triangleq \left[\begin{array}{c:cc} B & \begin{matrix}1&0\\1&0\\1&0\\1&0\end{matrix} \\ & \begin{matrix}0&1\\0&1\\0&1\\0&1\end{matrix} \end{array}\right] \qquad 4.2.21$$

$$\underline{\mu}_T \triangleq \left[\begin{array}{c} \underline{\mu} \\ \hdashline t^b{}_1 \\ \hdashline t^b{}_2 \end{array}\right]$$

and B, $\underline{\Delta t}$ and $\underline{\mu}$ are as defined in equations 4.2.22, 2.28, and 2.9 respectively.

The equation 4.2.20 is solved for $\hat{\underline{\mu}}_T$ by a pseudo inverse

$$\hat{\underline{\mu}}_T = (B_T^T B_T)^{-1} B_T^T \underline{\Delta t} \qquad 4.2.23$$

As with the extended algorithm for the velocity bias there is no computational advantage with a weighted version of this algorithm.

The computation requirements are presented in Table 4.2. There is an increase in computation for this algorithm, which estimates 5 parameters, over the velocity bias estimation algorithm which estimates 3 parameters, and the basic algorithm which estimates 3 parameters. This is because matrix computations, such as multiplications and Gaussian elimination, tend to increase as the cube of the size of the matrix.

The noise sensitivity of the algorithm extended for driver measurement bias is calculated similarly to that of the algorithm extended for velocity bias. As in equation 4.2.14, the covariance matrix for $\underline{\mu}_T$ is given by

$$P_T = (B_T^T B_T)^{-1} \sigma_n^2 \qquad 4.2.24$$

The rms value of the magnitude of the $\underline{\mu}$ when divided by σ_n is the noise sensitivity S_α of attitude estimates

$$S_\alpha = \sqrt{P_T(1,1) + P_T(2,2) + P_T(3,3)} \qquad 4.2.25$$

The variance of the two biases are given by the last two diagonal elements of P_T. Thus the noise sensitivities of t^b_1 and t^b_2 are respectively S_{b1} and S_{b2} where

Table 4.2 Computation Requirements for the Algorithm Extended for Driver Biases.

equation	times calculated	multiplies	divisions	add/subtracts	miscellaneous
2.1.3	2	18		12	
5.2.1	8	32		24	8 $\cos^{-1}$
5.2.4	1	80	8	40	8 square roots
$\underline{t} \cdot \underline{t}'$	1			8	
$B_T^T B_T$	1	200		175	
$B_T^T \underline{\Delta t}$	1	40		35	
Gaussian elimination	1	50	15	50	
2.2.2	1	18		18	
Gram Schmidt orthogonalization*		9	1	7	1 square root
Total		447	24	369	9 square roots, 8 $\cos^{-1}$

*averaged over three iterations

$$S_{b1} = \sqrt{P_T(4,4)} \qquad 4.2.26$$

$$S_{b2} = \sqrt{P_T(5,5)} \qquad 4.2.27$$

The sensitivities of α, t^b_1, and t^b_2 are computed as functions of platform attitude and transducer bias. For reasons expressed in section 4.2.1, the attitudes considered in the sensitivity computation, which are described by the Euler angle set (ϕ, θ, ψ), have ϕ, θ equal to 0, 0 and $\pi/4$, $\pi/4$' while all values of ψ between 0 and $\pi/4$ are included. The attitude sensitivity is shown in figure 4.6a for nominal values of the biases t^b_1, t^b_2 equal to 0, 0 and similarly S_{b1} and S_{b2} are shown in figure 4.5b.

The attitude sensitivity is about 10 percent higher than that of the basic algorithm. This increase will still meet system requirements. Analysis of this extended algorithm in comparison with the basic algorithm awaits further characterization of the biases and further study.

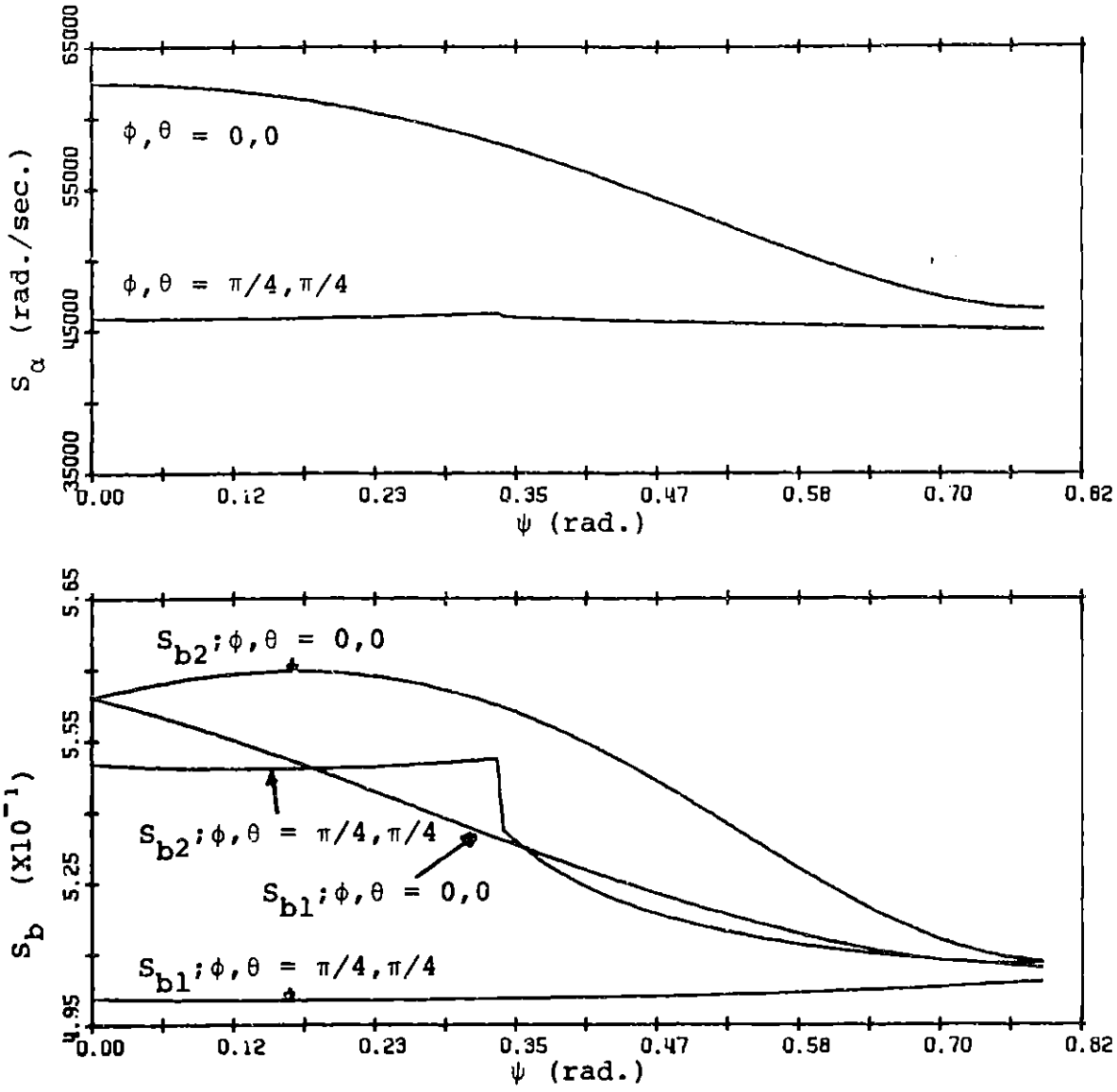

Figure 4.6 Noise Sensitivities of the Algorithm Extended for Driver Measurement Bias

V Conclusions and Suggestions for Further Study

5.1 Conclusions

In this thesis an algorithm for the estimation of the attitude of a floated inertial platform was developed. It is based on a linearization of a direction cosine system attitude model. This approach has enabled a reduction in computational requirement over the optimal approach of [3] while continuing to meet system specifications. Its computational requirements are typified by its multiplication count of 238 per attitude estimate while the previous nonlinear algorithm's multiplication requirement was estimated at over 2500 per attitude estimate. No study of actual computers for implementation of this algorithm has been made but it is believed that these requirements will not exceed the capacity of an airborne computer.

The algorithm's performance was analyzed in detail and compared with a simulation. These results showed the rms attitude error to be less than 0.75 milliradians. Defining a worst case error to be three times the rms value gives a worst case attitude error of 2.40 milliradians which is better than the specification of 2.91 milliradians.

An initialization procedure was developed to provide a nominal attitude required by the main algorithm upon startup due to its linearized formulation. A simulation of this procedure showed a maximum error which was sufficient to establish a nominal starting attitude.

The versatility of the algorithm developed in this thesis was demonstrated by the extension of the basic algorithm to include estimation of system parameters containing anticipated uncertainty. A sensitivity analysis of the extended algorithms showed only a minor decrease in performance from that of the basic algorithm, indicating that they would also meet the system requirements. A complete comparison of the extended and basic algorithms while subject to parameter uncertainty awaits further characterization of the uncertainty and further study.

5.2 Suggestions for Further Study

Further development would be able to decrease the computational requirements of the algorithm. Use of the same pseudoinverse, the calculation of which is half the total of the algorithm, for more than one attitude estimate w-uld trade linearization error for less computation. From the results of the performance analysis it appears that this would be possible for at least three estimates. Algorithm sensitivity could be traded for less computation by forming the estimator from fewer measurements.

The performance of the initialization procedure met system specifications. The heart of that procedure has a low computation requirement. However it requires much support, e.g., transducer selection. If there is no need for the versatility of the linearization approach and its better performance, an evaluation and reduction of the support to the initialization procedure could provide a main algorithm with a yet lower computational load.

Appendix A

Specifications

1. Radius of the case = 5.0 in.

2. Acoustic velocity in the case = 198,000 in./sec.

3. Maximum rotation of the inertial platform between measurements = 20 mrad. This is based on a maximum rotation rate of 2 rad./sec. and an interval of 10 msec. between measurements.

4. Worst case time measurement error = 3×10^{-8} sec.Assuming a Gaussian distribution, and the worst case representing a confidence level of 95% the RMS value of the time measurement noise is 1×10^{-8} sec.

5. Maximum allowable attitude error = 2.91 mrad. ($10\ \widehat{\text{min}}$). This error is the magnitude of a rotation relating the true and estimate attitudes. However, as the desired representation of estimated attitude is a direction cosine matrix (DCM) there may also be error in meeting the orthogonality constraints of a DCM, and then there is no pure rotation relating the true and estimate DCMs. In this case we will define the error ε to be the maximum length of a unit vector $\underline{v}$ transformed by an error matrix E which is the difference between the true DCM C and the estimate DCM $\hat{C}$.

$$\varepsilon = \max_{\underline{v}} | E \underline{v} | \qquad A.1$$

As defined above ε is the maximum singular value of E. Note that as the errors decrease the two definitions of error are asymptotically equivalent. This definition has the interpretation that if $\hat{C}_i^b$ is used to transform a unit vector v^i then the resultant vector $\hat{v}^b$ will contain an error vector of magnitude no greater than ε.

Appendix B

A Three Parameter Attitude Description

This appendix derives the expression for a direction cosine matrix C based on the three parameter description $\underline{\mu}$ from the expression based on the four parameter description $\alpha, \underline{\nu}$. As derived by Hutchinson in Appendix A of [3]

$$C = I + \sin \alpha \, N + (1-\cos \alpha) \, N^2 \qquad A1$$

where

$$N = \begin{bmatrix} 0 & -\nu_z & \nu_y \\ \nu_z & 0 & -\nu_x \\ -\nu_y & \nu_x & 0 \end{bmatrix} \qquad A2$$

The approach is to expand the functions of α, and combine them with the N matrices to form the M matrices.

$$M = \alpha N$$

First it is necessary to note that with $\underline{\nu}$ constrained to be unit length

$$N^3 = - N \qquad A4$$

$$N^4 = - N^2 \qquad A5$$

With these two relations any power of N has been expressed in N or N^2, and conversely,

$$N^{2M} = (-1)^{M-1} N^2 \qquad A6$$

$$N^{2M-1} = (-1)^{M-1} N \qquad A7$$

Equation A1 is expanded

$$C = I + \left[\alpha - \frac{\alpha^3}{3!} + \frac{\alpha^5}{5!} - \ldots\right]N + \left[\frac{\alpha^2}{2!} - \frac{\alpha^4}{4!} + \frac{\alpha^6}{6!}\ldots\right]N^2 \qquad A8$$

Applying equations A6 and A7 to equation A8

$$C = I + \left[\alpha N + \frac{\alpha^3}{3!} N^3 + \frac{\alpha^5}{5!} N^5 + \ldots\right] + \left[\frac{\alpha^2}{2!} N^2 + \frac{\alpha^4}{4!} N^4 + \frac{\alpha^6}{6!} N^6 \ldots\right] \qquad A9$$

Letting $\underline{\mu} = \alpha\underline{\nu}$, and consequently $M = \alpha N$, gives the desired result.

$$C = \sum_{k=o}^{\infty} \frac{M^k}{k!} \qquad A10$$

where

$$M^o = I$$

An alternative derivation can be obtained from the fact that a body's attitude described by a direction cosine matrix C when undergoing a rotation defined by the rotational velocity vector $\underline{\omega}$ must satisfy the following differential equation

$$\dot{C} = \Omega C$$

where

$$\Omega = \begin{bmatrix} 0 & -\omega_z & \omega_y \\ \omega_z & 0 & -\omega_x \\ -\omega_y & \omega_x & 0 \end{bmatrix}$$

For a constant $\underline{\omega}$ the solution to this equation over a time interval 0, T is

$$C = e^{\Omega T}$$

Defining

$$\underline{\omega} T = \underline{\mu}$$

gives the desired result

$$C = e^{M} = \sum_{k=0}^{\infty} \frac{M^K}{K!}$$

Appendix C

Update Error Calculations

This appendix will calculate the maximum singular values of the error matrices E_1 and E_2 where

$$E_1 = (\sin \alpha - \alpha)N + (1 - \cos \alpha)\, N^2 \qquad B1$$

$$E_2 = (\sin \alpha - \alpha)N + (1 - \cos \alpha - \frac{\alpha^2}{2})N^2 \qquad B2$$

$$N = \begin{bmatrix} 0 & -\nu_a & \nu_y \\ \nu_z & 0 & -\nu_x \\ -\nu_y & \nu_x & 0 \end{bmatrix} \qquad B3$$

$$\underline{\nu}^T \underline{\nu} = 1 \qquad B4$$

The singular values of E are the square roots of the eigenvalues of E^TE.

Letting

$$K_1 = \sin \alpha - \alpha \qquad B5$$

$$K_2 = 1 + \cos \alpha \qquad B6$$

$$K_3 = 1 - \cos \alpha - \frac{\alpha^2}{2} \qquad B7$$

$$E_1{}^T E_1 = (K_1 N + K_2 N^2)^T (K_1 N + K_2 N^2) \qquad B8$$

$$= (- K_1 N + K_2 N^2) (K_1 N + K_2 N^2) \qquad B9$$

$$= - K_1{}^2 N^2 + K_2{}^2 N^4 \qquad B10$$

Similarly

$$E_2{}^T E_2 = - K_1{}^2 N^2 + K_3{}^2 N^4 \qquad B11$$

The form of the matrix N combined with the constraint $|\underline{v}| = 1$ has the property that

$$N^4 = - N^2 \qquad B12$$

Thus

$$E_1{}^T E_1 = - (K_1{}^2 + K_2{}^2) N^2 \qquad B13$$

$$E_2{}^T E_2 = - (K_1{}^2 + K_3{}^2) N^2 \qquad B14$$

The eigenvalues of $E_1{}^T E_1$ are the solutions λ to

$$\text{Det} (- (K_1{}^2 + K_2{}^2) N^2 - I\lambda) = 0 \qquad B15$$

Define

$$\lambda' = \frac{\lambda}{K_1^2 + K_2^2} \qquad \text{B16}$$

Then expanding equation B15 and rearranging it

$$2\lambda'^2 (\nu_x^2 + \nu_y^2 + \nu_2^2) - \lambda' (\nu_x^2 + \nu_y^2 + \nu_z^2)^2 - \lambda' = 0 \qquad \text{B17}$$

Since $\underline{\nu}$ is unit length

$$\lambda'^3 - 2\lambda'^2 + \lambda' = 0 \qquad \text{B18}$$

$$\lambda' = 0,1 \qquad \text{B19}$$

$$\lambda = 0, (K_1^2 + K_2^2)$$

The maximum singular value ℓ_1, of E_1, is thus

$$\ell_1 = \sqrt{K_1^2 + K_2^2} = \sqrt{(\sin \alpha - \alpha)^2 + (1 - \cos \alpha)^2} \qquad \text{B20}$$

Similarly the maximum singular value ℓ_2, of E_2 is

$$\ell_2 = \sqrt{K_1^2 + K_3^2} = \sqrt{(\sin \alpha - \alpha)^2 + (1 - \cos \alpha - \frac{\alpha^2}{2})^2} \qquad \text{B21}$$

Appendix D

An Expression for the Rotation Between Two Attitudes Expressed as Quaternions

This appendix derives a formula for the magnitude α_3 of the rotation between two attitudes described by α_1, $\underline{\nu}_1$ and α_2, $\underline{\nu}_2$ where the α_i are rotation angles and the $\underline{\nu}_i$ are unit vectors representing rotation axes.

To enable use of Hamilton's quaternion algebra the attitudes must be described in a quaternion form λ, $\underline{\mu}$ where

$$\lambda = \cos \frac{\alpha}{2} \qquad \text{D1}$$

$$\underline{\mu} = \sin \frac{\alpha}{2} \underline{\nu}. \qquad \text{D2}$$

The rotation $\lambda_3, \underline{\mu}_3$ between $\lambda_1, \underline{\mu}_1$ and λ_2, $\underline{\mu}_2$ is the rotation formed by first rotating by λ_1, $\underline{\mu}_1$ and then by the inverse rotation of λ_2, $\underline{\mu}_2$ which is $-\lambda_2$, $\underline{\mu}_2$. From the quaternion algebra [2], [5]

$$\lambda_3 = - \lambda_1 \lambda_2 - \underline{\mu}_1 \cdot \underline{\mu}_2 \qquad \text{D3}$$

$$\underline{\mu}_3 = \lambda_1 \underline{\mu}_2 - \lambda_2 \underline{\mu}_1 + \underline{\mu}_2 \times \underline{\mu}_1 \qquad \text{D4}$$

There are two basic ways of solving for α_3:

$$\alpha_3 = 2 \cos^{-1} \lambda_3 \qquad \text{D5}$$

$$\alpha_3 = 2 \sin^{-1} |\underline{\mu}_3| \qquad \text{D6}$$

The equation of D6 is used to avoid small angle computational sensitivity of the inverse cosine at $\alpha_3 = 0$. Thus from equations D1, D2, D4 and D6 the desired expression is

$$\alpha_3 = 2\sin^{-1}|\cos\frac{\alpha_1}{2}\sin\frac{\alpha_2}{2}\underline{\nu}_2 - \cos\frac{\alpha_2}{2}\sin\frac{\alpha_1}{2}\underline{\nu}_1 + \sin\frac{\alpha_1}{2}\sin\frac{\alpha_2}{2}\,\underline{\nu}_2 \times \underline{\nu}_1|$$

Appendix E

Relationships Between Nine and Four Parameter Attitude Descriptions

The relationship between two orthogonal right handed coordinate frames that share a common origin is a rotation. A single rotation, of some magnitude α about some principle axis $\underline{\nu}$, of one frame will cause it to coincide with the other. Thus if the former frame is a reference then α and $\underline{\nu}$ describe the attitude of the latter body fixed frame. This is a four parameter description of the rotation as $\underline{\nu}$ is a three dimensional unit rector.

An equivalent representation of the rotation by a DCM,C is derived by Hutchinson in Appendix A of (3) as

$$C = I + \sin\alpha\, N + (1 - \cos\alpha)\, N^2 \qquad \text{F1}$$

where

$$N = \begin{bmatrix} 0 & -\nu_z & \nu_y \\ \nu_z & 0 & -\nu_z \\ -\nu_y & \nu_x & 0 \end{bmatrix} \qquad \text{F2}$$

The inverse relation is derived from the expansion of equation F1.

$$C = \begin{bmatrix} 1-(1-\cos\alpha)(\nu_y^2+\nu_z^2) & -\nu_z\sin\alpha+\nu_x\nu_y(1-\cos\alpha) & \nu_y\sin\alpha+\nu_x\nu_z(1-\cos\alpha) \\ \nu_z\sin\alpha+\nu_x\nu_y(1-\cos\alpha) & 1-(1-\cos\alpha)(\nu_x^2+\nu_z^2) & -\nu_x\sin\alpha+\nu_y\nu_z(1-\cos\alpha) \\ -\nu_y\sin\alpha+\nu_x\nu_z(1-\cos\alpha) & \nu_x\sin\alpha+\nu_y\nu_z(1-\cos\alpha) & 1-(1-\cos\alpha)(\nu_x^2+\nu_y^2) \end{bmatrix}$$

$$2 \sin \alpha \, \underline{\nu} = \begin{bmatrix} C_{32} - C_{23} \\ C_{13} - C_{31} \\ C_{21} - C_{12} \end{bmatrix} \triangleq \underline{\ell}$$

Now α may be expressed in terms of the differences between the off diagonal elements, $\underline{\ell}$.

$$|\ell| = 2 \sin\alpha \, |\underline{\nu}|$$

$$= 2 \sin\alpha$$

Thus

$$\alpha = \sin^{-1}(\tfrac{1}{2} \, |\ell|)$$

Once α is computed $\underline{\nu}$ is easily obtained

$$\underline{\nu} = \frac{\underline{\ell}}{2\sin\alpha}$$

This formula is not numerically sensitive for small angle rotations; but it is sensitive for α close to $\pi/2$. Then an alternative formula for α should be used based on the diagonal elements. The trace of C is

$$tr(C) = 3-(1-\cos\alpha)(2\nu_x^2+2\nu_y^2+\nu_z^2)$$

Since $\underline{\nu}$ is a unit vector

$$tr(C) = 3 - 2(1-\cos\alpha)$$

$$= 1 + 2\cos\alpha$$

Solving for α gives

$$\alpha = \cos^{-1}(\tfrac{1}{2}(tr(C)-1))$$

References

1. Hand, J.A., "AIRS System Description Book", Draper Laboratory Report C-4785, Cambridge, Mass., January 1974.

2. Gardner, R.A., "System Description of the Magnetostrictive Attitude Reference System (MARS)", Draper Laboratory Internal Memorandum 78-15G-244, December 1978.

3. Bonda, G.A., "Attitude Determination Using Static Estimation Procedures", Draper Laboratory Report T-673, October 1978.

4. McKern, R.A., "A Study of Transformation Algorithms for Use in a Digital Computer", Draper Laboratory Report T-493, January 1968.

5. Gelb, A., Applied Optimal Estimation, MIT Press, Cambridge, Mass., 1974.

6. Papoulis, A., Probability, Random Variables, and Stochastic Processes, McGraw Hill, New York, 1965.

7. Van Trees, H.L., Detection, Estimation and Modulation Theory, Part I, John Wiley and Sons, New York, 1968.

8. Penrose, R., "On the Best Approximate Solutions of Linear Matrix Equations", Proc. Cambridge Phil. Soc. Vol. 52, 1956.

9. Pease, M.C. Methods of Matrix Algebra Acedemic Press, New York, 1965.